iScience

CellPress
OPEN ACCESS

Article

Lifelong dietary omega-3 fatty acid suppresses thrombotic potential through gut microbiota alteration in aged mice

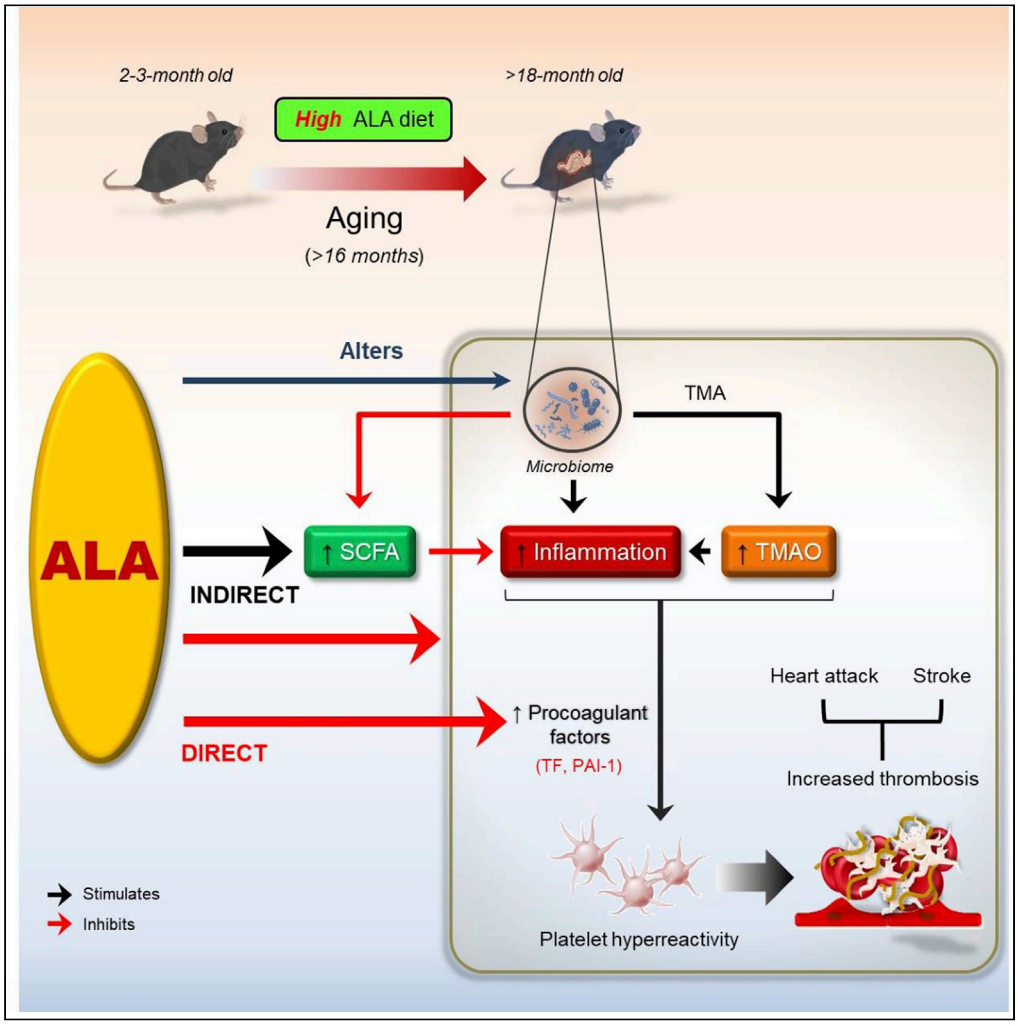

Seyed Soheil Saeedi Saravi, Nicole R. Bonetti, Benoit Pugin, ..., Thomas F. Lüscher, Giovanni G. Camici, Jürg H. Beer

hansjuerg.beer@ksb.ch

Highlights

Gut microbiota-derived TMAO and SCFAs associate with thrombotic potential in aging

Lifelong dietary ALA suppresses thrombus formation in aged mice

ALA-rich diet regulates aged gut microbiota and its metabolites TMAO and acetate

ALA-rich diet dampens inflammatory state in aged mice

Saeedi Saravi et al., iScience 24, 102897
August 20, 2021 © 2021 The Authors.
https://doi.org/10.1016/j.isci.2021.102897

iScience

CellPress
OPEN ACCESS

Article

Lifelong dietary omega-3 fatty acid suppresses thrombotic potential through gut microbiota alteration in aged mice

Seyed Soheil Saeedi Saravi,[1,2] Nicole R. Bonetti,[1,2] Benoit Pugin,[3] Florentin Constancias,[3] Lisa Pasterk,[1] Sara Gobbato,[2] Alexander Akhmedov,[4] Luca Liberale,[4,5] Thomas F. Lüscher,[4,6] Giovanni G. Camici,[4,7,8] and Jürg H. Beer[1,2,9,*]

SUMMARY

Aging is a major risk factor for cardiovascular diseases, including thrombotic events. The gut microbiota has been implicated in the development of thrombotic risk. Plant-derived omega-3 fatty acid α-linolenic acid (ALA) confers beneficial anti-platelet and anti-inflammatory effects. Hence, antithrombotic activity elicited by ALA may be partly dependent on its interaction with gut microbiota during aging. Here, we demonstrate that lifelong dietary ALA decreases platelet hyperresponsiveness and thrombus formation in aged mice. These phenotypic changes can be partly attributed to alteration of microbial composition and reduction of its metabolite trimethylamine N-oxide and inflammatory mediators including TNF-α, as well as the upregulated production of short-chain fatty acid acetate. ALA-rich diet also dampens secretion of increased procoagulant factors, tissue factor and plasminogen activator inhibitor-1, in aged mice. Our results suggest long-term ALA supplementation as an attractive, accessible, and well-tolerated nutritional strategy against age-associated platelet hyperreactivity and thrombotic potential.

INTRODUCTION

Aging is accompanied by multiple biological alterations (Niccoli and Partridge, 2012; Engbers et al., 2010) that induce functional changes in diverse cells resulting in an increased incidence of thrombotic complications in the elderly. Arterial thrombotic events, such as heart attack and stroke, remain the leading cause of morbidity and mortality worldwide. Platelet hyperreactivity and subsequent arterial thrombus formation are essential for end-organ injuries in atherothrombotic disease (Zhu et al., 2012; Chen et al., 2008). Platelet hyperreactivity and thrombosis risk are known to increase with aging which is associated with atherothrombosis (Le Blanc and Lordkipanidzé, 2019). On the other hand, accumulating evidence suggest that alterations in the gut microbiome could play a crucial role in the pathogenesis of cardiovascular disease including arterial and venous thrombosis. These studies propose a gut-cardiovascular system axis to demonstrate a clinical utility for diet-gut microbiota-cardiovascular disease interplay (Trøseid et al., 2020). The gut microbiota has been shown to undergo extensive alteration across the lifespan, and aging process may influence the gut microbiota and its metabolites. Importantly, an altered gut microbiota has been seen in aged patients with major adverse cardiovascular events and may explain some age-associated cardiovascular complications such as thrombosis (Kiouptsi et al., 2018). Given that currently available information indicate that the gut microbiota changes with age (DeJong et al., 2020), it remains unclear how or to what degree these changes may link to platelet hyperactivity and thrombotic potential. Altered composition of microbial communities, as characterized by increased production of metaorganismal metabolite trimethylamine N-oxide (TMAO), plays a critical causal link to stimulation of the process of platelet hyperreactivity and thrombosis (Reiner et al, 2017, 2019; Zhu et al., 2016; Tang et al., 2013). Therefore, alterations in the abundance of specific microbial communities may uncover the mechanisms by which aging modulates thrombosis.

During the past decade, diverse microbiome-targeted therapeutic strategies in cardiometabolic diseases from pre-/pro-biotic therapy to fecal microbiome transplantation have been explored, among them, a diet-

[1]Laboratory for Platelet Research, Center for Molecular Cardiology, University of Zurich, 8952 Schlieren, Switzerland

[2]Department of Internal Medicine, Cantonal Hospital Baden, Im Ergel 1, 5404 Baden, Switzerland

[3]Laboratory of Food Biotechnology, Institute of Food, Nutrition and Health, Department of Health Sciences and Technology, ETH Zurich, 8092 Zurich, Switzerland

[4]Center for Molecular Cardiology, University of Zurich, 8952 Schlieren, Switzerland

[5]Department of Internal Medicine, University of Genoa, Genoa, Italy

[6]Royal Brompton and Harefield Hospitals and Imperial College, London, UK

[7]University Heart Center, Department of Cardiology, University Hospital Zurich, Zurich, Switzerland

[8]Department of Research and Education, University Hospital Zurich, Zurich, Switzerland

[9]Lead contact

*Correspondence: hansjuerg.beer@ksb.ch

https://doi.org/10.1016/j.isci.2021.102897

This is an open access article under the CC BY-NC-ND license (http://creativecommons.org/licenses/by-nc-nd/4.0/).

based nutritional supplementation plays a critical role to improve gut microbial dysbiosis and restore a healthy microbiome configuration (Trøseid et al., 2020; Tang et al., 2019). Short-chain, plant-derived omega-3 poly-unsaturated fatty acid (PUFA), alpha-linolenic acid (ALA, 18:3 n-3) have been claimed for health benefits — to prevent cardiometabolic diseases and thrombotic events — which are supported by evidence from experimental and clinical trials (Bonetti et al., 2021; Reiner et al., 2017; Stivala et al., 2013). Our recent findings have demonstrated the beneficial anti-platelet effects of a diet supplemented with ALA on *in vivo* mouse models of arterial thrombosis and atherosclerosis (Stivala et al., 2020; Winnik et al., 2011; Holy et al., 2011). PUFA-rich diet counteracts inflammation and protects healthy metabolic state (Caesar et al., 2015; Oh et al., 2010; Calder, 2006), whereas saturated fatty acids promote inflammatory responses in diverse organs, leading to metabolic diseases (Kennedy et al., 2009). Moreover, supplementation with omega-3 PUFA has been shown to differentially modulate microbiome composition (Djuric et al., 2019; Calder, 2019), for instance, through a relative increase in abundance of genera *Bifidobacterium* and *Lactobacillus*, as well as a reduction in *Enterobacteriaceae* abundance (Watson et al., 2018; Younge et al., 2017). Conversely, n-3 PUFA deficiency drives impairment of short-chain fatty acid (SCFA) generation followed by gut dysbiosis (Robertson et al., 2017).

Therefore, based on prior findings, we hypothesized that lifelong dietary omega-3 ALA intake attenuates age-associated platelet hyperresponsiveness and heightened thrombus formation via alteration of gut microbial composition and derived metabolites, alongside the suppression of procoagulant responses.

RESULTS

Aging enhances platelet responsiveness to multiple agonists and thrombotic potential

We first investigated whether aging impacts platelet responsiveness to multiple agonists, the activation or expression of procoagulant surface receptors, as well as, thrombotic potential. We analyzed whole blood from healthy young (8–12 weeks) or old (>18 months) C57BL/6J mice and demonstrated remarkably higher values of platelet count and mean platelet volume (MPV), but not red or white blood cells, compared to young mice ($p < 0.05$ and $p < 0.01$, respectively; Table S1). Platelet-rich plasma (PRP) was then isolated from young or old mice, and effects of aging on platelet activation by multiple agonists ADP, collagen, and TRAP-6, as monitored by platelet aggregometry, was examined. An enhanced aggregometry response to increasing levels of ADP, collagen, or TRAP-6 in PRPs obtained from old compared with young mice was observed (Figures 1A–1F). PRP from old mice showed a maximum ADP-induced aggregation of 55% vs. 31% (1.25 μM, $p < 0.05$), 72% vs. 52% (2.5 μM, $p < 0.05$), and 77% vs. 61% (5 μM) compared with PRPs from young mice (n = 8–9, Figures 1A and 1B). In response to collagen, old PRP demonstrated increasing maximal aggregation of 62.59% vs. 41% (2.5 μg/mL), 81.87% vs. 49% (5 μg/mL, $p < 0.05$), and 79.99% vs. 58% (10 μg/mL) of aggregation compared with young PRP (n = 8–9, Figures 1C and 1D). Similarly, a significant enhancement of maximal aggregation was shown in response to stimulation with increasing doses of TRAP-6 (1.5, 3, and 5 μM) in old *versus* young PRPs (n = 8–9; Figures 1E and 1F). Moreover, the PRP preparations from old mice showed significant increases in the rate of platelet aggregation (inclination) in the presence of distinct agonists collagen of 10 μg/mL ($p < 0.05$), ADP of 1.25 μM ($p < 0.05$), and TRAP-6 of 1.3–5 μM ($p < 0.01$ and $p < 0.05$), when compared with PRP from young mice.

Flow cytometric analyses for PAC-1 binding showed significant increase in response to stimulation with low (0.1 U/ml) or high (0.5 U/ml) levels of thrombin in old versus young mice (n = 9–11, $p < 0.05$; Figure 1G). Similarly, the expression of GPIb, von Willebrand factor (vWF) receptor, and P-selectin, adhesion molecule, significantly enhanced with elderly (n = 9–11, $p < 0.05$; Figures 1H and 1I), likely contributing to the heightened platelet hyperresponsiveness to multiple agonists seen in old mice. To dissect the association between aging and procoagulant state, we performed proteome profiler array and exhibited an age-dependent increase in tissue factor (TF) and activated plasminogen activator inhibitor-1 (PAI-1), which converts normal anticoagulant endothelium into a procoagulant surface (Dielis et al., 2005), in old compared with young mice (Figure 1J). Consistently, these results were confirmed upon proof of the association between aging and thrombotic potential: platelet adhesion to vWF-coated surfaces within whole blood obtained from young or old mice was analyzed under high-shear flow (100 dyn/cm^2) and showed significant elevations in platelet-covered area at t = 5 min (37.04%) in old compared with young mice (n = 8–9, $p < 0.01$; Figures 1K and 1L). Collectively, aging illustrated a direct association with increased platelet activation and aggregability, as well as thrombosis risk in an *ex vivo* shear-induced thrombosis model.

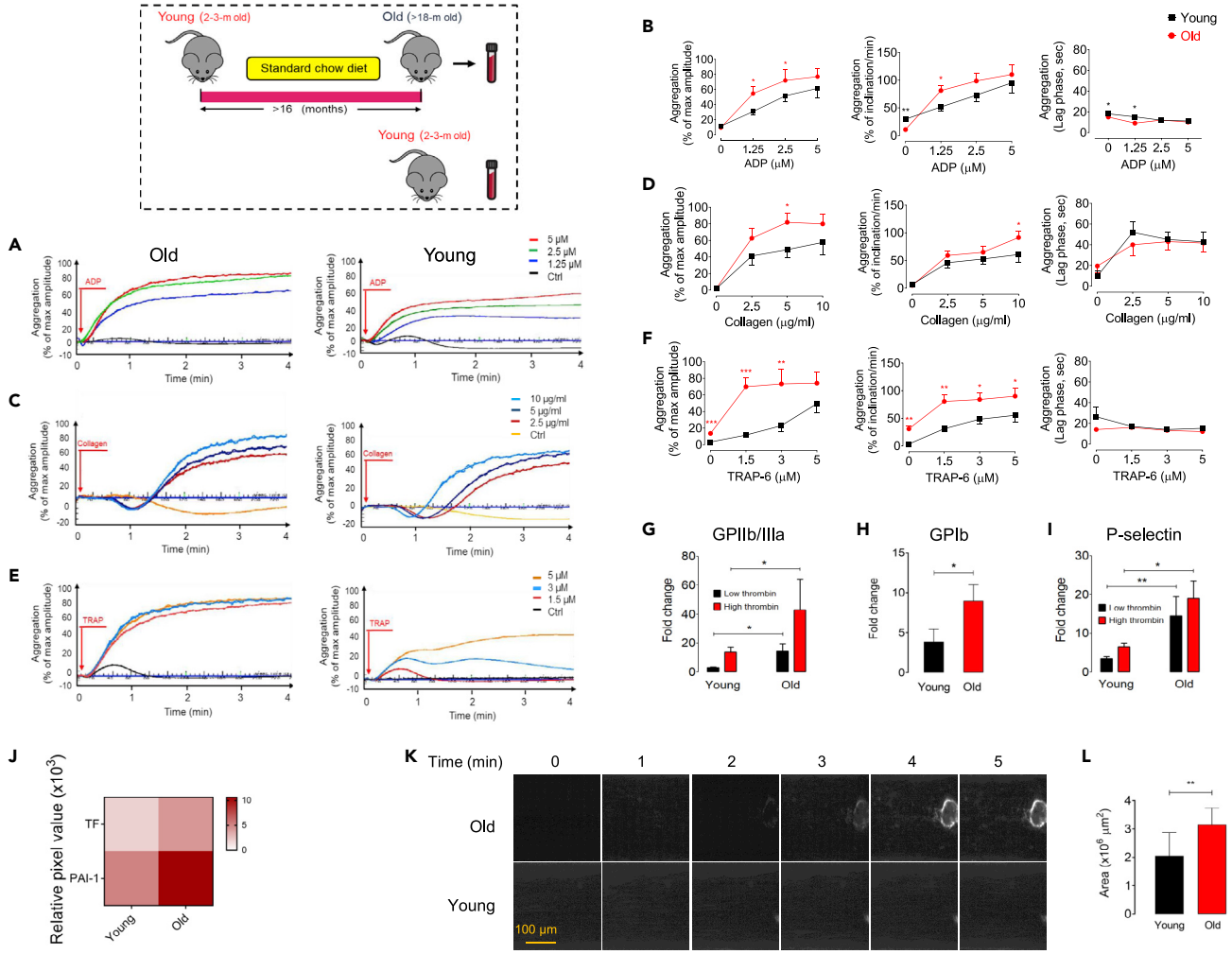

Figure 1. Aging promotes platelet hyperreactivity and thrombotic potential

(A–I) Representative curves of platelet aggregation in healthy young (8–12 weeks, n = 9; lower panels) and old (>18 months, n = 8; upper panels) mice in response to stimulation with specific doses of (A) ADP (1.25, 2.5, and 5 µM), (C) collagen (2.5, 5, and 10 µg/mL), and (E) TRAP-6 (1.5, 3, and 5 µM) for 4 min (B, D, F). These bar plots represent % maximal aggregation, % inclination (slope), and lag time. Platelet activation analysis by flow cytometry of washed platelets from young or old mice (n = 9) stimulated with low (0.1 IU/mL) or high (0.5 IU/mL) doses of thrombin as determined by activation of procoagulant surface receptors (G) GPIIb/IIIa and (H) GPIb, or (I) expression of P-selectin. These experiments were independently repeated three times with similar results.

(J) Heatmap depicting plasma procoagulants TF and PAI-1 fold changes measured by multiplex proteome array in young versus old mice (n = 8–9) developed by chemiluminescence.

(K) Representative images of platelet adhesion and thrombus formation over a von Willebrand factor (vWF)-coated microfluidic chamber under high-shear conditions (100 dyn/cm^2) for 5 min in whole blood obtained from either young or old mice (n = 9); Scale bar: 100 µm.

(L) Shown are the pooled data analyzing adherent platelet area per square micrometer of chamber surface at t = 5 min. All values are presented as mean ± S.D. *p < 0.05, **p < 0.01, ***p < 0.001. Red arrows indicate the times of drug addition.

Aging induces shifts in the gut microbial composition and modulates TMAO and SCFAs production and inflammatory responses

Here, we sought to assess whether aging induces shifts in the gut microbial composition that could affect thrombotic potential, at least in part, through alteration of gut microbiota-derived TMAO and SCFAs. Analysis of the gut microbial composition within young and old mice using 16S rRNA gene metabarcoding followed by principal coordinate analysis (PCoA) revealed that age induces a dramatic rearrangement in the fecal microbial community structure based on Aitchison community dissimilarity (Figure 2A). PERMANOVA exhibited that age explained 30.5% of total variability in microbiota community structure, defined as beta-diversity (R^2 = 0.30, p = 0.002; Figure 2A), whereas no significant differences in microbial community

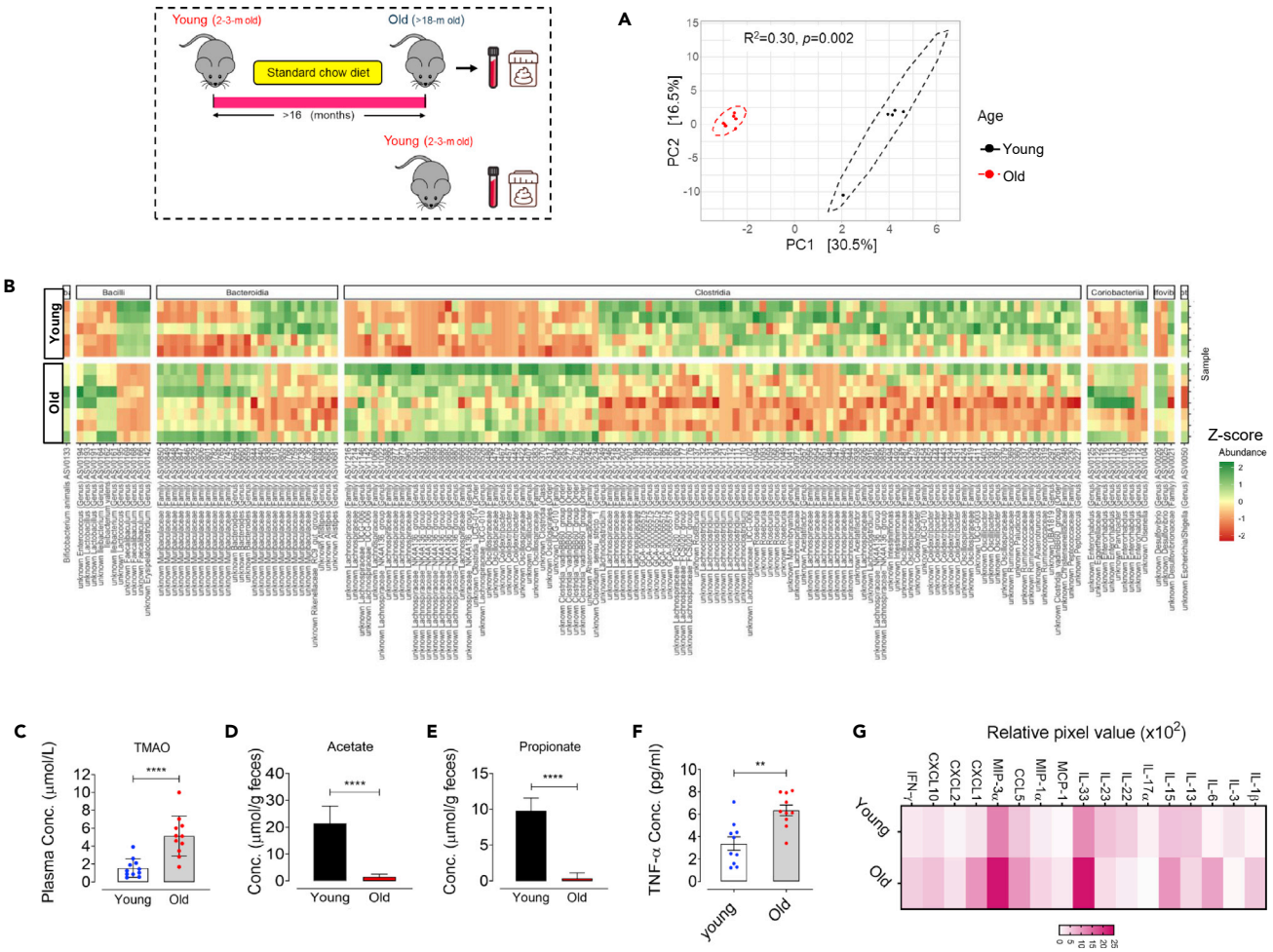

Figure 2. Aging alters microbial community composition and metabolites TMAO and SCFAs, and aggravates inflammatory responses

(A) Principal coordinate analysis plot comparing beta-diversity of gut microbiota structure in young or old mice (n = 5–7).

(B) Heatmap depicting all ASV differentially abundant (row *Z* score; $p < 0.05$) in the feces of young *versus* old mice (n = 5–7); See also Data S1.

(C–E) Quantification of plasma TMAO levels and SCFAs acetate and propionate per gram feces within healthy young *versus* old mice (n = 11).

(F and G) (F) Quantification of plasma TNF-α levels (n = 10) and (G) multiplex plasma inflammatory cytokines and chemokines array developed by chemiluminescence, in young *versus* old mice (n = 8–9). **$p < 0.01$, ****$p < 0.0001$.

alpha-diversity was observed between young *versus* old mice (Figure S1). Aging conferred no significant alteration in phylum-level relative abundance in the feces from old or young mice (data not shown), yet a higher *Firmicutes/Bacteroidota* ratio was seen in young compared with old mice ($p = 0.042$; Figure S1). At family-level, aging was seen to associate with remarkable decreases in the proportion of *Streptococcaceae*, *Peptococcaceae*, *Ruminococcaceae*, *Oscillospiraceae*, *Rikenellaceae*, and increases in *Staphylococcaceae*, *Clostridiaceae*, *Anaerovoracaceae*, *Bacteroidaceae*, and *Muribaculaceae* (Figure S1). Specifically, a total of 162 amplicon sequence variant (ASV) were differentially abundant among young and old mice (Figure 2B, Data S1, FDR adjusted p values <0.05 based on DESeq2 negative binomial tests), thereby highlighting the important rearrangement of the gut microbial community with aging. Old mice showed a significant reduction in the genera *Faecalibaculum*, which counteracts inflammatory state and negatively associates with major proinflammatory cytokines TNF-α, IL-1β, and IL-6 (Zhu et al., 2020a, 2020b), *Rikenellaceae_RC9_gut_group*, a taxonomic group which is associated with a healthy metabolic state (Zheng et al., 2018; Ijaz et al., 2018; Lippert et al., 2017), and in the butyrate-producing and anti-inflammatory *Oscillospiraceae (Intestinimonas)* (Li et al., 2020; Bui et al., 2015). Importantly, lactic acid bacteria *Lactococcus*, known as a probiotic to correlate with anti-inflammatory and health benefits, decreased in old compared with young mice (Cook et al., 2018; Luerce et al., 2014). In similar analyses, the genus

Peptococcaceae, identified to both negatively contribute to TMAO levels and *in vivo* clot formation, was remarkably decreased in old mice versus young mice (Zhu et al., 2016). As shown in Figure 2B, aging was associated with a significant increase in the proportions of *Desulfovibrio*, known for producing trimethylamine (TMA), a precursor of TMAO (Zeisel and Warrier, 2017), and for modulating the production of proinflammatory cytokines (Zhang-Sun et al., 2015), and of genera *Ileibacterium*, in particular *I. valens*, a genus which is highly abundant in the intestinal microbiota of mice with heart failure (Khannous-Lleiffe et al., 2020). In line, these taxonomic shifts were accompanied by age-dependent alteration in microbiota-derived metabolites levels, so that age is known to be both significantly positively associated with plasma TMAO levels ($p < 0.0001$, Figure 2C) and negatively associated with fecal levels of SCFAs, acetate, and propionate, seen in old *versus* young mice (for both $p < 0.0001$, Figures 2D and 2E).

Moreover, we executed plasma inflammatory profiling in old *versus* young mice and revealed that aging exacerbates plasma TNF-α levels in old mice ($p < 0.05$, Figure 2F). Consistently, we found a remarkable elevation in other major proinflammatory cytokines, including interleukin-1β (IL-1β) and IL-6, as well as, secretion of chemokines monocyte chemoattractant protein-1 (MCP-1), macrophage inflammatory protein-3α (MIP-3α), and CXCL1 (Figure 2G). Taken together, these results show an association between the gut microbiota compositional shifts during aging and inflammatory imbalance signals and thrombotic phenotype.

The gut microbial metabolite TMAO dose-dependently exacerbates platelet hyperresponsiveness

To confirm the impact of microbiota-derived TMAO on thrombotic potential, we assessed platelet hyperresponsiveness to multiple agonists ADP, collagen, and TRAP-6 in presence of increasing levels of exogenous TMAO (10, 30, and 100 μM). Platelet aggregation was exacerbated by treatment with exogenous TMAO in a dose-dependent manner (Figure 3), and a significant increase in maximal aggregation in response to TMAO at 10 μM ($p < 0.05$) and 30 μM ($p < 0.01$) by stimulation with submaximal levels of ADP (2.5 μM), collagen (5 μg/mL), and TRAP-6 (3 μM) was observed. Moreover, a remarkably increased rate of platelet aggregation, determined as higher percent inclination and shorter lag time, was observed in TMAO-incubated PRPs stimulated by submaximal dose of TRAP-6 ($p < 0.05$ for % of inclination in response to 30 and 100 μM of TMAO; $p < 0.01$ for lag time in response to 10 and 30 μM of TMAO).

ALA suppresses age-promoted *ex vivo* thrombus generation

We further exploited a nutritional strategy with ALA supplementation to attenuate age-dependent enhanced thrombus formation. In the present study, C57BL/6J mice were maintained on a chemically defined either low (0.03% w/w, n = 9) or high (7.3% w/w) ALA-supplemented diet for >16 months. Dietary high ALA intake significantly increased platelet count ($p < 0.05$) and MPV ($p < 0.001$) in old mice (Table S1). The high ALA diet elicited no differences in multiple indices of platelet activation, including procoagulant surface receptors GPIIb/IIIa, GPIb, and P-selectin in low or high levels of thrombin-stimulated washed platelets obtained from old mice (Figures 4C–4E). Moreover, to test whether high ALA diet affects procoagulant state, we performed proteome profiler array, and showed a remarkable decrease in plasma levels of procoagulant factors TF and activated PAI-1 in old mice fed a high *versus* low ALA diet (Figure 4F). We next examined the effect of lifelong ALA-rich diet on platelet adhesion to vWF, a pivotal player in platelet adhesion and aggregation at high-shear conditions (Spiel et al., 2008). Figure 4A shows representative images of vWF-coated microfluidic chamber under shear flow with whole blood from old mice fed a low or high ALA diet at initial (t = 0) and subsequent 5 min interval period. Platelet adherence and thrombus rate of formation were quantified, as shown in Figures 4A and 4B. High ALA diet significantly ($p < 0.05$) decreased the heightened platelet thrombus formation on the vWF-coated surface within whole blood obtained from old mice, whereas no antithrombotic role was seen for low ALA diet (Figures 4A and 4B). As can be seen in Figure 4A, the rate of fluorescent thrombus formation was decreased in old mice fed high ALA versus low ALA. Cumulatively, the above data demonstrate that lifelong dietary high ALA intake suppresses age-associated thrombus formation, although a negligible effect was seen on platelet activation.

Lifelong dietary ALA differentially affects the gut microbiota and ameliorates both TMAO and SCFAs levels and inflammatory mediators

To determine the specific effects of lifelong dietary ALA intake on the gut microbiota, the microbial composition was analyzed by 16S rRNA gene metabarcoding, and the microbial function was assessed by

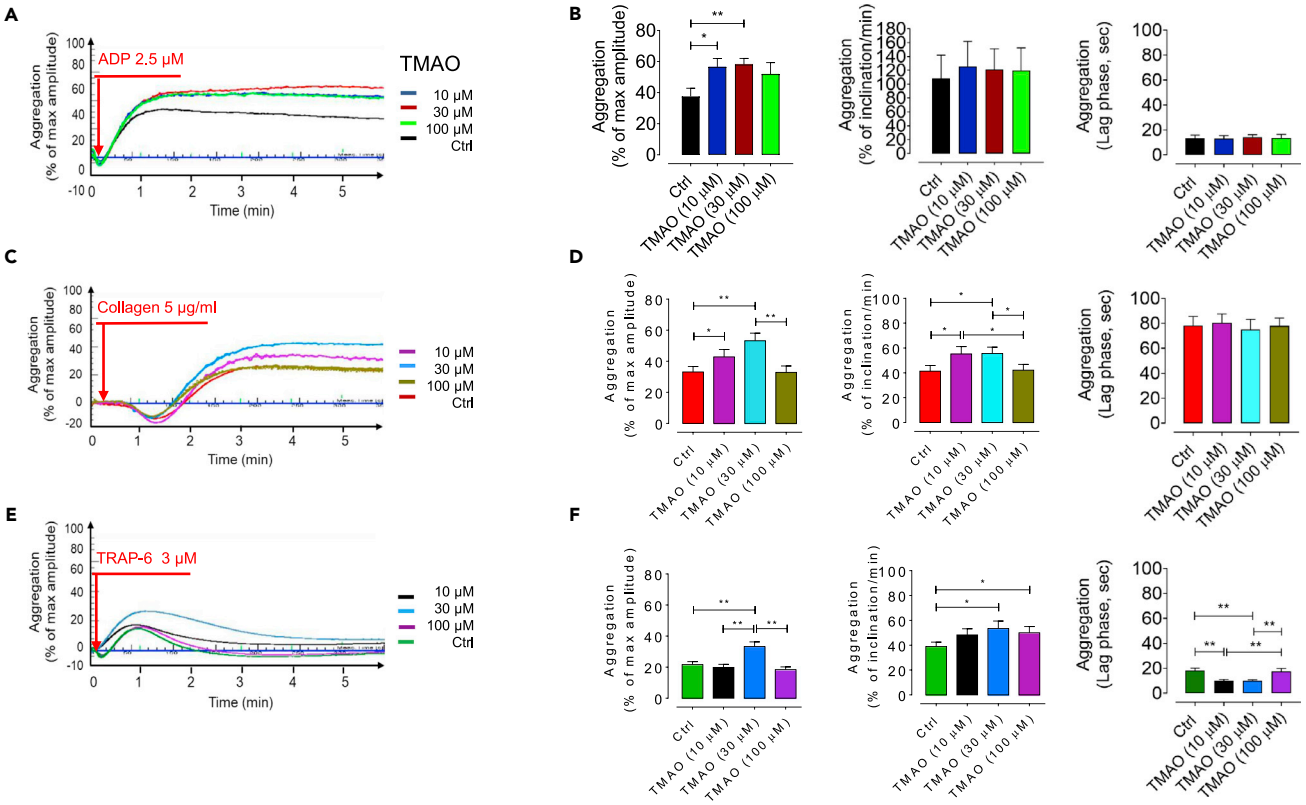

Figure 3. TMAO dose-dependently exacerbates platelet hyperresponsiveness

Platelet aggregation in TMAO-pretreated blood (10, 30, and 100 µM, for 1 hr) taken from healthy young (8–12 weeks, n = 9) mice in response to stimulation with submaximal concentrations of (A) ADP (2.5 µM), (C) collagen (5 µg/mL), and (E) TRAP-6 (3 µM) for 4 min (B, D, F). These bar plots represent pooled data showing % maximal aggregation, % inclination (slope), and lag time. All values are presented as mean ± S.D. Red arrows indicate the times of drug addition. *p < 0.05, **p < 0.01.

quantifying plasma TMAO and fecal SCFAs levels. Community structure, as using PCoA based on Aitchison distance, revealed a clear and significant clustering of samples according to diet with 28.9% variability in microbial community structure within old mice fed a low or high ALA diet (R^2 = 0.27, p = 0.002; Figure 5A). Lifelong high ALA-rich diet induced significant changes of alpha-diversity of the microbial communities with decreased Faith's phylogenetic richness (PD; FDR adjusted p = 0.023) and increased phylogenetic clustering of the ASV (SES.MPD, FDR adjusted p = 0.015) in old mice, whereas no significant alteration was seen in observed richness and Shannon's diversity indices (Figure S2). A total of 119 ASV were differentially abundant among old mice fed a high or low ALA diet (Figure 5B, Data S2; FDR adjusted p < 0.05), emphasizing a remarkable effect of high ALA intake on gut microbial community, although no significant alteration was observed in phylum-level abundance (data not shown) nor in *Firmicutes/Bacteroidota* ratio (p = 0.56; Figure S2). Among a multitude of taxa that were impacted by dietary high ALA, the proportional abundance of *Ruminococcaceae* UCG-010, *Marinifilaceae*, and *Clostridiaceae* were significantly reduced (Figure S2). The genera *Clostridia_sensu_stricto_1*,*_VadinBB60 group* and *Tyzzerella* –all belonging to the *Clostridiaceae* family — were significantly reduced within high ALA-fed old mice (Figures 5B and S2). Our results show a decrease in the abundance of *Lachnoclostridium*, a genus which is positively associated with TMAO production (Tabata et al., 2021; Jameson et al., 2016), and enriched in patients with atrial fibrillation (Tabata et al., 2021) and heart failure with preserved ejection fraction (HFpEF) (Lvovich et al., 2020), in the microbiota from old mice fed a high ALA compared with low ALA diet (Figure 5B). Moreover, *Bilophila*, a genus which is aggravated in response to high-fat diet (HFD) (Natividad et al., 2018), was increased when treated with high ALA diet (Figures 5B and S2), suggesting that fatty acid supplementation could promote the growth of yet poorly characterized lipophilic bacteria (Agans et al., 2018). Compared with low ALA diet, *Desulfovibrio* (Figure 5B), a genus that associate with increased plasma TMAO levels (Fu et al., 2020) and production of inflammatory cytokines (Zhang-Sun et al., 2015) and Anaerovorax, which

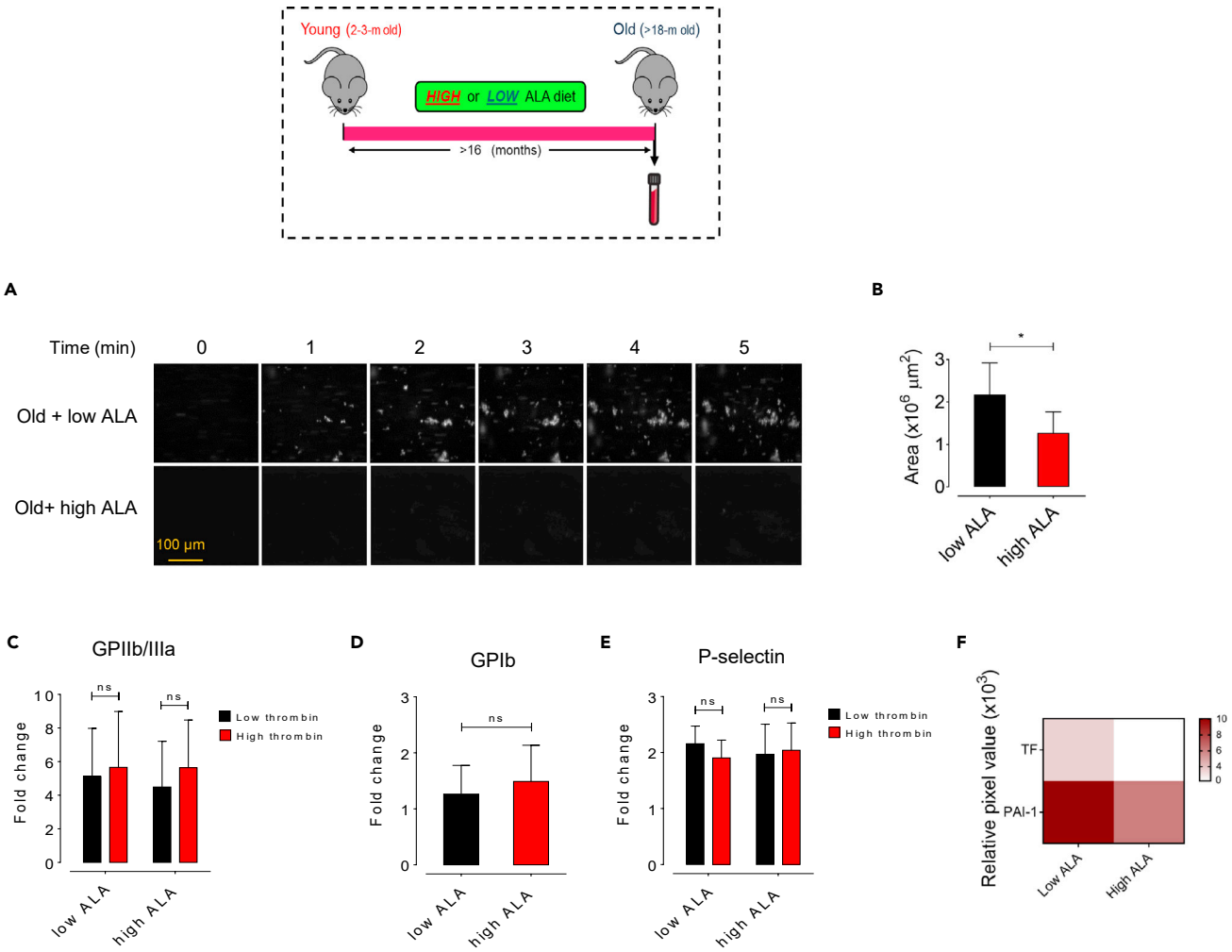

Figure 4. Lifelong dietary ALA suppresses aging-linked thrombosis

(A and B) Representative images illustrating platelet adhesion over a vWF-coated microfluidic chamber under high-shear conditions (100 dyn/cm^2) for 5 min in whole blood obtained from either young or old mice fed low (0.03%) or high (7.3%) doses of ALA for at least 16 months (n = 8), expressed as adherent platelet area/µm^2 of chamber surface at t = 5 min; Scale bar: 100 µm.

(C–E) Platelet activation analysis by flow cytometric analysis of platelet hyperreactivity in low or high-fed old mice (n = 8–9) in response to stimulation with low or high thrombin as determined by activation of platelet (C) GPIIb/IIIa and (D) GPIb, and (E) expression of surface P-selectin.

(F) Heatmap depicting plasma procoagulants TF and PAI-1 fold changes measured by multiplex proteome array in old mice fed a dietary low or high ALA for >16 months (n = 8–9) developed by chemiluminescence. All values are presented as mean ± S.D. *p < 0.05, **p < 0.01.

observed to mediate inflammation and lipid metabolism abnormalities (Yuan et al., 2020; Figure S2), as well as diverse members of the family *Lachnospiraceae* (particularly, *Acetatifactor*, *Lachnospiraceae_FCS020_group*, *Lachnospiraceae_NK4A136*, and *Eisenbergiella* groups), were strikingly reduced in old mice fed a high ALA diet. Consistently, dietary supplementation with high ALA (>16 months) induced a remarkable decrease in plasma TMAO levels in old mice ($p < 0.05$; Figure 5C), whereas fecal level of SCFA acetate, but not propionate, was significantly increased in high *versus* low ALA-fed old mice ($p < 0.05$; Figures 5D and 5E). Notably, the influence of high ALA diet on TMAO production correlated to decreased plasma levels of choline — but not betaine — which is an essential dietary precursor for the TMA production (Figure S4).

To identify taxonomic markers associated with the reduction of age-associated thrombosis risk, we assessed whether dietary high ALA modulates aged microbial communities toward a youthful enterotype. Overall, high ALA diet did not promote a community structure as similar as young mice;

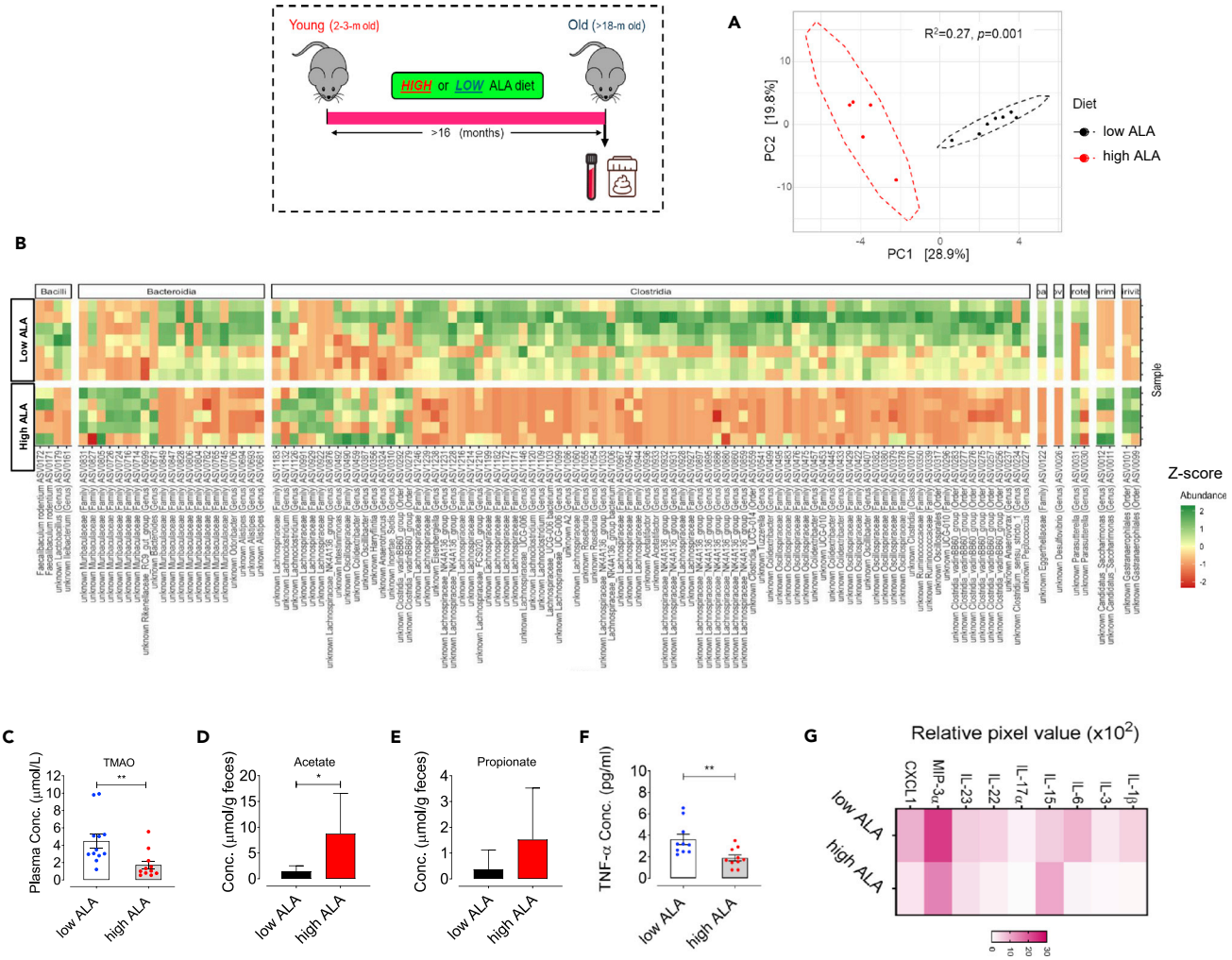

Figure 5. Dietary ALA regulates TMAO and SCFAs levels and inflammatory state by differential modulation of the gut microbiota

(A) Principal coordinate analysis of beta-diversity of the gut microbiome within old mice fed low or high ALA diet (n = 5–7).

(B) Heatmap depicting all ASV differentially abundant (row *Z* score; $p < 0.05$) in the feces of low *versus* high ALA-fed old mice (n = 5–7); See also Data S1.

(C–E) Quantification of plasma TMAO levels and SCFAs acetate and propionate per gram feces within old mice fed low or high ALA diet for >16 months (n = 7–12).

(F and G) (F) Quantification of plasma TNF-α levels (n = 10) and (G) multiplex plasma inflammatory cytokines and chemokines array developed by chemiluminescence, in old mice fed a lifelong dietary low *versus* high ALA for >16 months (n = 8–9). *$p < 0.05$, ns, no significance.

nevertheless, 7 ASVs (for instance, health-promoting and TMA-reducing *Rikenellaceae_RC9_gut_group* and *Intestinimonas*, which were reduced in the aging, could be partially restored by high ALA diet (Figure S3). On the other hand, high ALA dramatically reduced 32 age-dependently high abundant ASVs, including TMA-producing and inflammation-driving *Desulfovibrio*, TMAO- and HFD-associated Clostridium genera (Zhu et al., 2020a, 2020b) *Clostridia_sensu_stricto_1* (Zhu et al., 2020a, 2020b; Hoyles et al., 2018), *Clostridium_UCG-014, and Clostridia_vadinBB60_group* (Koeth et al., 2013), heart failure-associated *Ileibacterium*, and *Lachnospiraceae* (*Lachnospiraceae_NK4A136_group Lachnospiraceae_UCG-006*), which are found more abundant in a rat model of HFD (Zhao et al., 2019; Data S1 and S2).

To test whether lifelong high ALA diet could attenuate inflammation during aging, we performed plasma inflammatory profiling in old mice (n = 8–9, Figures 5F and 5G). Old mice that fed a high ALA diet showed a remarkable lower plasma TNF-α concentration ($p > 0.01$; Figure 5F) and other proinflammatory cytokines IL-1β and IL-6 than old mice fed a low ALA diet, whereas an increase was seen in immunoregulatory

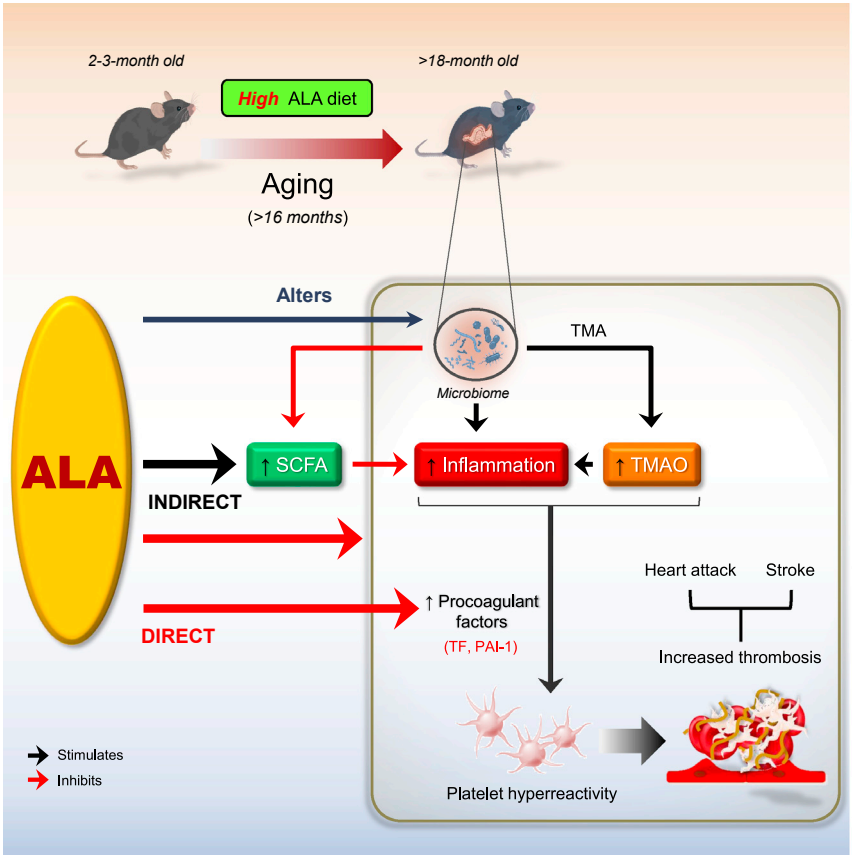

Figure 6. Schematic illustrating the benefits of lifelong dietary ALA for the suppression of age-associated atherothrombotic events

The scheme illustrates a metaorganismal pathway showing that lifelong nutritional supplementation with ALA attenuates platelet hyperresponsiveness and enhanced thrombotic risk both directly through the reduction of procoagulant factors and indirectly through the modulation of the gut microbiota and its metabolites TMAO and SCFA acetate, as well as the suppression of inflammatory responses in aged mice. ALA, α-linolenic acid; SCFA, short-chain fatty acid; TMA, trimethylamine; TMAO, trimethylamine N-oxide. Black arrow indicates *stimulation*; Red arrow indicates *inhibition*. See text for details.

cytokine IL-15 in high ALA-fed old mice (Figure 5G). Moreover, high ALA diet elicited a decrease in the secretion of MIP-3α — a small protein that modulates innate immune system and upregulates inflammatory cytokines TNF-α and IFN-γ (Hoover et al., 2002) — and CXCL1 — an inflammatory and prothrombotic mediator involved in inflammasome activation and subsequent IL-1β production in macrophages (Boro and Balaji, 2017) — within old mice compared with old mice that fed a low ALA diet (n = 8–9; Figure 5G). Taken together, these data strongly suggest that lifelong ALA-rich diet can suppress inflammatory state and specific gut microbial taxa, which are associated with the production of microbial metabolite TMAO and the subsequent thrombosis risk during the aging.

DISCUSSION

The present study, for the first time, reports the interesting findings that lifelong dietary ALA regulates age-associated platelet hyperreactivity and thrombotic potential. Additionally, this study expands our understanding that lifelong n-3 ALA-rich diet beneficially modulates the aged gut microbiota which is associated, at least in part, with the inflammatory response and dysregulation of metaorganismal metabolites TMAO and SCFAs during aging (Figure 6). We found that old mice fed a lifelong ALA-rich diet are protected against age-associated procoagulant and inflammatory state, which is associated with platelet hyperreactivity and enhanced thrombus formation under high-shear conditions. Our current studies demonstrated that lifelong dietary ALA increased the aged fecal microbiome diversity and was both negatively associated

with TMAO generation and positively associated with the production of SCFA acetate. Consistent with previous studies showing that gut microbiota composition reciprocally can be shaped by nutrients from diet (Witkowski et al., 2020; Ziętak et al., 2016; Chevalier et al., 2015; Dey et al., 2015; Kau et al., 2011; Turnbaugh et al., 2008), we show that age and type of diet (high *versus* low ALA) are two major determinants of the composition and diversity of the gut microbiota.

Our results from 16S rRNA gene metabarcoding analyses show that lifelong supplementation with high ALA could simultaneously reduce the abundance of *Desulfovibrio*, sulfate-reducing bacteria which has been linked to TMA production and the subsequent thrombosis (Zhu et al., 2016) and to TLR4-mediated inflammation processes that lead to metabolic diseases (Zhang-Sun et al., 2015) and some genera belonging to the family *Ruminococcaceae*, which are positively associated with TMA production and atherosclerosis in humans and negatively associated with *in vivo* arterial occlusion time (Ascher and Reinhardt, 2017; Wang et al., 2015; Bäckhed, 2013). A reduction was observed in *Clostridia_sensu_stricto_1*, *_VadinBB60 group*, and *Tyzzerella*, which are mostly abundant in the dysbiotic microbiota and linked to enhanced expression of proinflammatory cytokines and TLR3 and intestinal inflammation (Zou et al., 2020; Burrello et al., 2018) and to increased cardiovascular disease risk (Wang et al., 2017; Kelly et al., 2016), in high ALA-fed old mice, whereas *Clostridia_VadinBB60 group* was enriched in the gut microbiota from old mice. Moreover, a concomitant increase in genera *Intestinimonas*, a butyrate-producing genus which contributes to anti-inflammatory responses and maintenance of healthy gut and cardiovascular system (Li et al., 2020; Zuo et al., 2019; Bui et al., 2015), was seen in response to lifelong dietary high ALA intake in old mice. Our results suggested that lifelong ALA-rich diet suppresses the enhanced platelet hyperresponsiveness during aging likely though alteration of TMA-associated gut microbial genera and reduction of TMAO (Figure 6), which is previously shown to be negatively linked to thrombotic potential *in vivo* in mice and ADP-dependent platelet aggregation responses in humans (Roberts et al., 2018; Zhu et al., 2016; Wang et al., 2011). Fish oil has been shown to decrease plasma concentration of choline, precursor for TMA, and suppresses TMAO production. It accelerates TMAO metabolism via regulating liver flavin monooxygenase-3 (FMO3) activity involved in fatty acid oxidation and subsequently decreases plasma TMAO concentration (Yu et al., 2017). These data are consistent with our findings that show a significantly decreased plasma choline and TMAO concentrations in old mice fed a lifelong high ALA diet compared with low ALA diet. Concerning the multifactorial nature and major role of the gut microbiome in TMAO production, limiting the TMA-enriched food (consisting choline, L-carnitine, Betaine, and Trimethyl-L-lysine (TML), which is present in significant quantities in seafood-, red meat-, and dairy products-rich diet) in diet, manipulation of the gut microbiota, and inhibition of FMO3 activity are considered as certain strategies in order to decrease circulating TMAO levels and prevent its negative cardiovascular outcome (Simó and García-Cañas, 2020). Here, omega-3 fatty acid ALA alters the abundance of both TMA-producing and -lowering genera and likely decreases FMO3 activity through which decreases plasma TMAO levels in old mice.

Consistent with a recent study (Lee et al., 2020), we showed that the fecal SCFAs decrease ~80% in old mice, whereas SCFA acetate is restored and may be positively associated with declined platelet hyperreactivity and clot formation in high ALA-fed old mice (Figure 6). These findings are coherent to prior studies demonstrating that omega-3 PUFAs, including DHA, restore natural balance between the gut microbiota and mucosal immune system and positively correlate with production of SCFAs independent of fiber metabolism (Menni et al., 2017; Costantini et al., 2017). To date, there is no evidence of a direct link between the gut microbiota-derived metabolite SCFAs and thrombotic events, although some animal studies point that fecal SCFAs directly negatively associate with inflammation and cardiovascular diseases, including atherosclerosis and blood pressure (Verhaar et al., 2020; Bartolomaeus et al., 2019). For instance, SCFA propionate has been shown to execute a potent anti-inflammatory effect on $CD4^+$ T cell function and protect from angiotensin II-induced vascular inflammation and atherosclerosis (Bartolomaeus et al., 2019; Ohira et al., 2017). SCFAs are also widely known to inhibit histone deacetylase, which may contribute to the expression of cytokines in T immune cells (Arpaia et al., 2013). Acetate and propionate promote the polarization of $CD4^+$ T cells into Th1 and Th17 effector cells that generate immunoregulatory cytokines e.g. IL-10 (Park et al., 2015). We, here, elucidate that dietary high ALA modulates aged microbial communities toward a youthful-like enterotype that returns to an increase in proportion of taxa which are associated with healthy state and generation of SCFAs acetate, propionate and butyrate, e.g. *Rikenellaceae_RC9_gut_group* (Wang et al., 2020; Song et al., 2018) and *Intestinimonas* (Bui et al., 2020; Louis and Flint 2017), and to a drastically reduction in age-dependently

high abundant genera that contribute to TMAO production and inflammatory response, e.g. *Desulfovibrio*.

Our current results showed that high ALA reduces the age-dependently increased secretion of procoagulant factors TF and PAI-1, which were associated with most prethrombotic disease conditions and directly with thrombotic risk (Figure 6; Reiner et al., 2017; Breitenstein et al., 2010; Yamamoto et al., 2005). Body of evidences revealed that both PAI-1 and TF reflect TMAO in senescent human umbilical venous endothelial cells (HUVEC; Ke et al., 2018) and primary human coronary artery endothelial cells (HCAECs) through activation of NF-κB-mediated signaling pathway (Cheng et al., 2019), respectively. Increased release of PAI-1 from activated platelets in platelet-rich arterial thrombi has shown that PAI-1 also reflects inflammatory stimuli (Tjärnlund-Wolf et al., 2012). Altogether, the elevated plasma levels of TF and PAI-1 could result from the increased levels of TMAO and proinflammatory cytokines, particularly TNF-α, seen in aged mice. These findings are consistent with our previous study that indicates TNF-α induced endothelial TF expression and activity through activation of MAP kinases (Holy et al., 2011). This association is likely confirmed where a reduced secretion of the procoagulant factors in high ALA-fed old mice is along with a decreased level of TMAO and inflammatory mediators. Considering prior studies, marine n–3 fatty acids EPA and DHA dampen inflammation through both partial replacement of arachidonic acid, the substrate for biosynthesis of proinflammatory eicosanoids, in the cell membranes (Calder, 2019), and interference to the expression of NF-κB-mediated genes encoding proinflammatory cytokines and adhesion molecules (Djuric et al., 2019; Calder, 2015, 2017). Moreover, omega-3 fatty acids could also reverse the inflammatory effects of high-saturated-fat diet that might be elicited by microbial restoration, thereby downregulating proinflammatory TLR signaling and blocking intestinal permeability to endotoxins (Caesar et al., 2015; Lam et al., 2015). Omega-3 fatty acids also inhibit HFD-induced NLRP3 inflammasome activation and the subsequent caspase-1 activation and IL-1β secretion (Yan et al., 2013). We previously showed that ALA supplementation of 8-week old *ApoE*$^{-/-}$ mice for 16 weeks reduces the expression of TNF-α and TNF-α-positive area on atherosclerotic plaques (Winnik et al., 2011). Our current data provide evidence that there is likely a link between altered gut microbiota composition and anti-inflammatory effects of high ALA diet. Indeed, lifelong dietary ALA decreased some genera belonging to the phyla *Proteobacteria* including *Desulfovibrio* and *Firmicutes* including *Clostridia_VadinBB60 group*, which both are known to be positively associated with inflammatory responses during aging process (Fu et al., 2020; Zou et al., 2020; Burrello et al., 2018; Conley et al., 2016). Based on the current findings that a lifelong high ALA diet could decrease plasma TMAO levels within old mice and on our previous studies showing that ALA interferes with clustering of GPIb receptors on platelet surface under high-shear rates (Stivala et al., 2020), we indicate that ALA may modulate both directly, via amelioration of platelet reactivity and adhesion to vWF and decrease in procoagulant factors, and indirectly, via the reduction of TMAO production and inflammatory cytokines and increase in SCFA acetate.

In summary, our observations highlight that lifelong supplementation with a high ALA diet reverses age-associated platelet hyperreactivity and heightened thrombotic potential (Figure 6). A critical question answered by these studies is the identification of putative mechanisms that underlie antithrombotic effects of lifelong dietary high ALA, including the regulation of metaorganismal metabolites TMAO and SCFA acetate, inflammatory cytokines, and procoagulant factors TF and PAI-1. The strength of this study is the utilization of long-term (lifelong) nutritional approach using an ALA-rich diet to attenuate thrombotic risk during aging that is coherent with partial alteration of the aging gut microbiota toward TMAO-lowering, anti-inflammatory, and antithrombotic state and regulation of microbial metabolites and inflammatory response in aged mice. Therefore, the study proposes a long-term ALA-rich diet as an attractive, cheap, abundantly available, and non-toxic nutritional strategy that potentially can prevent age-associated thrombotic events.

Limitations of the study

Altogether, we explored not fully the associations between specific microbial genera and metaorganismal including TMAO and SCFAs. Moreover, our knowledge which microbial genera are correlated to inflammatory responses in aged mice is still limited. Our further *in vitro* studies on single microbial genera and their byproducts will shed light to answer these questions. Blood sampling via cardiac puncture, in which animals are bled to death, limits our lifelong studies of each single mouse during aging. We, therefore, designed our groups as follows: Young; Old; Old + lifelong low ALA; Old + lifelong high ALA. The sampling also

provides a limited volume of whole blood samples that limits assessment of the bioavailability and metabolism of ALA and the distribution of ALA and its long-chain n-3 FA metabolites. All mice were obtained from the same colony and kept under the same and permanent conditions for proper inter-group comparisons. On the other hand, a lifelong nutritional strategy in mice, for obvious logistical reasons, limits translational extrapolation to human studies. Nevertheless, our recent long-term studies of patients with atrial fibrillation (Swiss Atrial Fibrillation Cohort Study (Swiss-AF); (Bertschi et al., 2021) has shown an inverse association of omega-3 fatty acids with D-dimer, indicating a reduced procoagulant response and the subsequent stroke (Reiner et al., 2021) and thromboembolic disorders (Wu et al., 2015). Thus, further long-term nutritional supplementation with ALA in aged humans may likely confirm our current findings that long-term dietary ALA confers antithrombotic effects in aged mice.

STAR★METHODS

Detailed methods are provided in the online version of this paper and include the following:

- KEY RESOURCES TABLE
- RESOURCE AVAILABILITY
  - Lead contact
  - Materials availability
  - Data and code availability
- EXPERIMENTAL MODEL AND SUBJECT DETAILS
- METHOD DETAILS
  - Platelet-rich plasma and washed platelet preparation
  - Blood analysis
  - Platelet aggregometry assay
  - Whole blood *ex vivo* thrombosis assay
  - Platelet flow cytometry
  - Proteome profiler array
  - ELISA of mice plasma
  - LC–MS/MS analysis of mouse plasma samples
  - 16S rRNA gene amplicon sequencing and bioinformatic processing
  - Quantitative SCFA analysis
- QUANTIFICATION AND STATISTICAL ANALYSIS

SUPPLEMENTAL INFORMATION

Supplemental information can be found online at https://doi.org/10.1016/j.isci.2021.102897.

ACKNOWLEDGMENTS

This work was supported by funds from the Swiss National Science Foundation grant #310030_144152 to J.H.B.

AUTHOR CONTRIBUTIONS

S.S.S.S., N.R.B., L.P., S.G., A.A., G.G.C., and J.H.B. designed the experiments. S.S.S.S., N.R.B., L.P., S.G., A.A., and L.L. performed the experiments, including mouse studies, microfluidic and platelet-related studies, cytokine arrays, and flow cytometry. S.S.S.S. and N.R.B. analyzed all data. B.P. and F.C. performed bioinformatics and statistical analysis of 16S metabarcoding data and SCFA measurements. G.G.C., and T.F.L., and B.P. contributed to manuscript. S.S.S.S. and J.H.B. drafted and wrote the manuscript. J.H.B. obtained the funding and designed the project.

DECLARATION OF INTERESTS

The authors declare no competing interests.

Received: April 20, 2021
Revised: June 17, 2021
Accepted: July 20, 2021
Published: August 20, 2021

REFERENCES

Agans, R., Gordon, A., Kramer, D.L., Perez-Burillo, S., Rufián-Henares, J.A., and Paliy, O. (2018). Dietary fatty acids sustain the growth of the human gut microbiota. Appl. Environ. Microbiol. *84*, e01525-18.

Anders, S., and Huber, W. (2010). Differential expression analysis for sequence count data. Gen. Biol. *11*, R106.

Arpaia, N., Campbell, C., Fan, X., Dikiy, S., van der Veeken, J., deRoos, P., Liu, H., Cross, J.R., Pfeffer, K., Coffer, P.J., et al. (2013). Metabolites produced by commensal bacteria promote peripheral regulatory T-cell generation. Nature *504*, 451–455.

Ascher, S., and Reinhardt, C. (2017). The gut microbiota: an emerging risk factor for cardiovascular and cerebrovascular disease. Eur. J. Immunol. *48*, 564–575.

Bäckhed, F. (2013). Meat-metabolizing bacteria in atherosclerosis. Nat. Med. *19*, 533–534.

Bartolomaeus, H., Balogh, A., Yakoub, M., Homann, S., Markó, L., Höges, S., Tsvetkov, D., Krannich, A., Wundersitz, S., Avery, E.G., et al. (2019). Short-chain fatty acid propionate protects from hypertensive cardiovascular damage. Circulation *139*, 1407–1421.

Bertschi, D.A., Reiner, M.F., Saeedi Saravi, S.S., Rutishauser, J., Werlen, L., Aeschbacher, S., Osswald, S., Conen, D., Beer, J.H. (2021). Association of Omega-3 fatty acids with D-Dimers and beta-thromboglobulin as a marker of coagulation activation in atrial fibrillation. 65th Meeting of the Society of Thrombosis and Haemostasis Research (GTH 2021).

Bonetti, N.R., Liberale, L., Akhmedov, A., Pasterk, L., Gobbato, S., Puspitasari, Y.M., Vukolic, A., Saeedi Saravi, S.S., Coester, B., and Horvath, C. (2021). Long-term dietary supplementation with plant-derived omega-3 fatty acid improves outcome in experimental ischemic stroke. Atherosclerosis *325*, 89–98.

Boro, M., and Balaji, K.N. (2017). CXCL1 and CXCL2 regulate NLRP3 inflammasome activation via G-protein-coupled receptor CXCR2. J. Immunol. *199*, 1660–1671.

Breitenstein, A., Camici, G.G., and Tanner, F.C. (2010). Tissue factor: beyond coagulation in the cardiovascular system. Clin. Sci. (Lond) *118*, 159–172.

Bui, T.P.N., Troise, A.D., Nijsse, B., Roviello, G.N., Fogliano, V., and de Vos, W.M. (2020). *Intestinimonas*-like bacteria are important butyrate producers that utilize *Nε*-fructosyllysine and lysine in formula-fed infants and adult. J. Func. Food *70*, 103974.

Bui, T., Ritari, J., Boeren, S., de Waard, P., Plugge, C.M., and de Vos, W.M. (2015). Production of butyrate from lysine and the Amadori product fructoselysine by a human gut commensal. Nat. Commun. *6*, 10062.

Burrello, C., Garavaglia, F., Cribiù, F.M., Ercoli, G., Lopez, G., Troisi, J., Colucci, A., Guglietta, S., Carloni, S., Guglielmetti, S., et al. (2018). Therapeutic faecal microbiota transplantation controls intestinal inflammation through IL10 secretion by immune cells. Nat. Commun. *9*, 5184.

Caesar, R., Tremaroli, V., Kovatcheva-Datchary, P., Cani, P.D., and Backhed, F. (2015). Crosstalk between gut microbiota and dietary lipids aggravates WAT inflammation through TLR signaling. Cell. Metab. *22*, 658–668.

Calder, P.C. (2006). n-3 polyunsaturated fatty acids, inflammation, and inflammatory diseases. Am. J. Clin. Nutr. *83*, 1505S–1519S.

Calder, P.C. (2015). Marine omega-3 fatty acids and inflammatory processes: effects, mechanisms and clinical relevance. Biochim. Biophys. Acta. *1851*, 469–484.

Calder, P.C. (2017). Omega-3 fatty acids and inflammatory processes: from molecules to man. Biochem. Soc. Trans. *45*, 1105–1115.

Calder, P.C. (2019). Is increasing microbiota diversity a novel anti-inflammatory action of marine n–3 fatty acids? J. Nutr. *149*, 1102–1104.

Callahan, B.J., McMurdie, P.J., Rosen, M.J., Han, A.W., Johnson, A.J.A., and Holmes, S.P. (2016). DADA2: high-resolution sample inference from Illumina amplicon data. Nat. Methods *13*, 581.

Chen, K., Febbraio, M., Li, W., and Silverstein, R.L. (2008). A specific CD36- dependent signaling pathway is required for platelet activation by oxidized low-density lipoprotein. Circ. Res. *102*, 1512–1519.

Cheng, X., Qiu, X., Liu, Y., Yuan, C., and Yang, X. (2019). Trimethylamine N-oxide promotes tissue factor expression and activity in vascular endothelial cells: a new link between trimethylamine N-oxide and atherosclerotic thrombosis. Thromb. Res. *177*, 110–116.

Chevalier, C., Stojanovi_c, O., Colin, D.J., Suarez-Zamorano, N., Tarallo, V., Veyrat-Durebex, C., Rigo, D., Fabbiano, S., Stevanovi_c, A., Hagemann, S., et al. (2015). Gut microbiota orchestrates energy homeostasis during cold. Cell *163*, 1360–1374.

Conley, M.N., Wong, C.P., Duyck, K.M., Hord, N., Ho, E., and Sharpton, T.J. (2016). Aging and serum MCP-1 are associated with gut microbiome composition in a murine model. Peer J *4*, e1854.

Cook, D.P., Gysemans, C., and Mathieu, C. (2018). Lactococcus lactis as a versatile vehicle for tolerogenic immunotherapy. Front. Immunol. *8*, 1961.

Costantini, L., Molinari, R., Farinon, B., and Merendino, N. (2017). Impact of omega-3 fatty acids on the gut microbiota. Int. J. Mol. Sci. *18*, 2645.

DeJong, D.N., Surette, M.G., and Bowdish, D.M.E. (2020). The gut microbiota and unhealthy aging: disentangling cause from consequence. Cell Host. Microbe *28*, 180–189.

Dey, N., Wagner, V.E., Blanton, L.V., Cheng, J., Fontana, L., Haque, R., Ahmed, T., and Gordon, J.I. (2015). Regulators of gut motility revealed by a gnotobiotic model of diet-microbiome interactions related to travel. Cell *163*, 95–107.

Dielis, A.W.J.H., Smid, M., Spronk, H.M.H., Hamulyak, K., Kroon, A.A., ten Cate, H., and de Leeuw, P.W. (2005). The prothrombotic paradox of hypertension. Hypertension *46*, 1236–1242.

Djuric, Z., Bassis, C.M., Plegue, M.A., Sen, A., Turgeon, D.K., Herman, K., Young, V.B., Brenner, D.E., and Ruffin, M.T. (2019). Increases in colonic bacterial diversity after ω-3 fatty acid supplementation predict decreased colonic prostaglandin E2 concentrations in healthy adults. J. Nutr. *149*, 1170–1179.

Engbers, M.J., van Hylckama Vlieg, A., and Rosendaal, F.R. (2010). Venous thrombosis in the elderly: incidence, risk factors and risk groups. J. Thromb. Haemost. *8*, 2105–2112.

Fu, B.C., Hullar, M.A.J., Randolph, T.W., Franke, A.A., Monroe, K.R., Cheng, I., Wilkens, L.R., Shepherd, J.A., Madeleine, M.M., Le Marchand, L., et al. (2020). Associations of plasma trimethylamine *N*-oxide, choline, carnitine, and betaine with inflammatory and cardiometabolic risk biomarkers and the faecal microbiome in the Multiethnic Cohort Adiposity Phenotype Study. Am. J. Clin. Nutr. *111*, 1226–1234.

Glöckner, F.O., Yilmaz, P., Quast, C., Gerken, J., Beccati, A., Ciuprina, A., Bruns, G., Yarza, P., Peplies, J., Westram, R., et al. (2017). 25 years of 516 serving the community with ribosomal RNA gene reference databases and tools. J. Biotechnol. *261*, 169–176.

Holy, E.W., Forestier, M., Richter, E.K., Akhmedov, A., Leiber, F., Camici, G.G., Mocharla, P., Luscher, T.F., Beer, J.H., and Tanner, F.C. (2011). Dietary alpha-linolenic acid inhibits arterial thrombus formation, tissue factor expression, and platelet activation. Arterioscler. Thromb. Vasc. Biol. *31*, 1772–1780.

Hoover, D.M., Boulegue, C., Yang, D., Oppenheim, J.J., Tucker, K., Lu, W., and Lubkowski, J. (2002). The structure of human macrophage inflammatory protein-3alpha/ CCL20. Linking antimicrobial and CC chemokine receptor-6-binding activities with human beta-defensins. J. Biol. Chem. *277*, 37647–37654.

Hoyles, L., Jiménez-Pranteda, M.L., Chilloux, J., Brial, F., Myridakis, A., Aranias, T., Magnan, C., Gibson, G.R., Sanderson, J.D., Nicholson, J.K., et al. (2018). Metabolic retroconversion of trimethylamine N-oxide and the gut microbiota. Microbiome *6*, 73.

Ijaz, M.U., Ahmed, M.I., Zou, X., Hussain, M., Zhang, M., Zhao, F., Xu, X., Zhou, G., and Li, C. (2018). Beef, casein, and soy proteins differentially affect lipid metabolism, triglycerides accumulation and gut microbiota of high-fat diet-fed C57BL/6J mice. Front. Microbiol. *9*, 1–13.

Jameson, E., Doxey, A.C., Airs, R., Purdy, K.J., Murrell, J.C., and Chen, Y. (2016). Metagenomic data-mining reveals contrasting microbial populations responsible for trimethylamine formation in human gut and marine ecosystems. Microb. Genom. *2*, e000080.

Kau, A.L., Ahern, P.P., Griffin, N.W., Goodman, A.L., and Gordon, J.I. (2011). Human nutrition, the gut microbiome and the immune system. Nature *474*, 327–336.

Ke, Y., Li, D., Zhao, M., Liu, C., Liu, J., Zeng, A., Shi, X., Cheng, S., Pan, B., Zheng, L., et al. (2018). Gut flora-dependent metabolite Trimethylamine-N-oxide accelerates endothelial cell senescence and vascular aging through oxidative stress. Free Rad. Biol. Med. *116*, 88–100.

Kelly, T.N., Bazzano, L.A., Ajami, N.J., He, H., Zhao, J., Petrosino, J.F., Correa, A., and He, J. (2016). Gut microbiome associates with lifetime cardiovascular disease risk profile Among bogalusa heart study participants. Circ. Res. *119*, 956–964.

Kennedy, A., Martinez, K., Chuang, C.-C., LaPoint, K., and McIntosh, M. (2009). Saturated fatty acid-mediated inflammation and insulin resistance in adipose tissue: mechanisms of action and implications. J. Nutr. *139*, 1–4.

Khannous-Lleiffe, O., Willis, J.R., Saus, E., Cabrera-Aguilera, I., Almendros, I., Farré, R., Gozal, D., Farré, N., and Gabaldón, T. (2020). Impact of sleep fragmentation, heart failure, and their combination, on the gut microbiome. BioRxiv. https://doi.org/10.1101/2020.09.11.294447.

Kiouptsi, K., Ruf, W., and Reinhardt, C. (2018). Microbiota-derived trimethylamine. Circ. Res. *123*, 1112–1114.

Koeth, R.A., Wang, Z., Levison, B.S., Buffa, J.A., Org, E., Sheehy, B.T., Britt, E.B., Fu, X., Wu, Y., Li, L., et al. (2013). Intestinal microbiota metabolism of L-carnitine, a nutrient in red meat, promotes atherosclerosis. Nat. Med. *19*, 576–585.

Lam, Y.Y., Ha, C.W., Hoffmann, J.M., Oscarsson, J., Dinudom, A., Mather, T.J., Cook, D.I., Hunt, N.H., Caterson, I.D., Holmes, A.J., and Storlien, L.H. (2015). Effects of dietary fat profile on gut permeability and microbiota and their relationship with metabolic changes in mice. Obesity *23*, 1429–1439.

Le Blanc, J., and Lordkipanidzé, M. (2019). Platelet function in aging. Front. Cardiovasc. Med. *6*, 109.

Lee, J., d'Aigle, J., Atadja, L., Quaicoe, V., Honarpisheh, P., Ganesh, B.P., Hassan, A., Graf, J., Petrosino, J., Putluri, N., et al. (2020). Gut microbiota–derived short-chain fatty acids promote poststroke recovery in aged mice. Circ. Res. *127*, 453–465.

Li, B., Li, L., Li, M., Lam, S.M., Wang, G., Wu, Y., Zhang, H., Niu, C., Zhang, X., Liu, X., et al. (2019). Microbiota depletion impairs thermogenesis of brown adipose tissue and browning of white adipose tissue. Cell. Rep. *26*, 2720–2737.

Li, W., Lu, L., Liu, B., and Qin, S. (2020). Effects of phycocyanin on pulmonary and gut microbiota in a radiation-induced pulmonary fibrosis model. Biomed. Pharmacother. *132*, 110826.

Lippert, K., Kedenko, L., Antonielli, L., Kedenko, I., Gemeier, C., Leitner, M., Kautzky-Willer, A., Paulweber, B., and Hack, E. (2017). Gut microbiota dysbiosis associated with glucose metabolism disorders and the metabolic syndrome in older adults. Benef. Microbes *8*, 545–556.

Louis, P., and Flint, H.J. (2017). Formation of propionate and butyrate by the human colonic microbiota. Environ. Microbiol. *19*, 29–41.

Luerce, T.D., Gomes-Santos, A.C., Rocha, C.S., Moreira, T.G., Cruz, D.N., Lemos, L., Sousa, A.L., Pereira, V.B., de Azevedo, M., Moraes, K., et al. (2014). Anti-inflammatory effects of Lactococcus lactis NCDO 2118 during the remission period of chemically induced colitis. Gut. Pathog. *6*, 33.

Lvovich, N.A., Nikolaevna, K.A., Sergeevna, P.M., Tsaler'evich, Z.B., Vladimirovich, P.S., Vladimirovna, Z.A., Evgenievna, F.Z., Rizoevna, M.T., Vasilievna, K.L., Dmitrievna, K.T., et al. (2020). Microbiome changes in patients with chronic heart failure with preserved ejection fraction correlate with fibrosis markers: description of a Russian cohort. Res. Square. https://doi.org/10.21203/rs.3.rs-94727/v1.

McMurdie, P.J., and Holmes, S. (2013). Phyloseq: an R package for reproducible interactive analysis and graphics of microbiome census data. PLoS One *8*, e61217.

Menni, C., Zierer, J., Pallister, T., Jackson, M.A., Long, T., Mohney, R.P., Steves, C.J., Spector, T.D., and Valdes, A.M. (2017). Omega-3 fatty acids correlate with gut microbiome diversity and production of N-carbamylglutamate in middle aged and elderly women. Sci. Rep. *7*, 11079.

Mueller, D.M., Allenspach, M., Othman, A., Saely, C.H., Muendlein, A., Vonbank, A., Drexel, H., and von Eckardstein, A. (2015). Plasma levels of trimethylamine-N-oxide are confounded by impaired kidney function and poor metabolic control. Atherosclerosis *243*, 638–644.

Natividad, J.M., Lamas, B., Pham, H.P., Michel, M.L., Rainteau, D., Bridonneau, C., da Costa, G., van Hylckama Vlieg, J., Sovran, B., and Chamignon, C. (2018). *Bilophila wadsworthia* aggravates high fat diet induced metabolic dysfunctions in mice. Nat. Commun. *9*, 2802.

Niccoli, T., and Partridge, L. (2012). Ageing as a risk factor for disease. Curr. Biol. *22*, R741–R752.

Oh, D.Y., Talukdar, S., Bae, E.J., Imamura, T., Morinaga, H., Fan, W., Li, P., Lu, W.J., Watkins, S.M., and Olefsky, J.M. (2010). GPR120 is an omega-3 fatty acid receptor mediating potent anti-inflammatory and insulin-sensitizing effects. Cell *142*, 687–698.

Ohira, H., Tsutsui, W., and Fujioka, Y. (2017). Are short chain fatty acids in gut microbiota defensive players for inflammation and atherosclerosis? J. Atheroscler. Thromb. *24*, 660–672.

Park, J., Kim, M., Kang, S.G., Jannasch, A.H., Cooper, B., Patterson, J., and Kim, C.H. (2015). Short-chain fatty acids induce both effector and regulatory T cells by suppression of histone deacetylases and regulation of the mTOR-S6K pathway. Mucosal Immunol. *8*, 80–93.

Poeker, S.A., Lacroix, C., de Wouters, T., Spalinger, M.A., Scharl, M., and Geirnaert, A. (2019). Stepwise development of an in vitro continuous fermentation model for the murine caecal microbiota. Front. Microbiol. *10*, 1–14.

Reiner, M.F., Baumgartner, P., Wiencierz, A., Coslovsky, M., Bonetti, N.R., Filipovic, M.G., Montrasio, G., Aeschbacher, S., Rodondi, N., Baretella, O., et al. (2021). The omega-3 fatty acid eicosapentaenoic acid (EPA) correlates inversely with ischemic brain infarcts in patients with atrial fibrillation. Nutrients *13*, 651.

Reiner, M.F., Müller, D., Gobbato, S., Stalder, O., Limacher, A., Bonetti, N.R., Pasterk, L., Méan, M., Rodondi, N., Aujesky, D., et al. (2019). Gut microbiota-dependent trimethylamine-N-oxide (TMAO) shows a U-shaped association with mortality but not with recurrent venous thromboembolism. Thromb. Res. *174*, 40–47.

Reiner, M.F., Stivala, S., Limacher, A., Bonetti, N.R., Méan, M., Egloff, M., Rodondi, N., Aujesky, D., von Schacky, C., Lüscher, T.F., et al. (2017). Omega-3 fatty acids predict recurrent venous thromboembolism or total mortality in elderly patients with acute venous thromboembolism. J. Thromb. Haemost. *15*, 47–56.

Roberts, A.B., Gu, X., Buffa, J.A., Hurd, A.G., Wang, Z., Zhu, W., Gupta, N., Skye, S.M., Cody, D.B., Levison, B.S., et al. (2018). Development of a gut microbe-targeted non-lethal therapeutic to inhibit thrombotic potential. Nat. Med. *24*, 1407–1417.

Robertson, R.C., Oriach, C.S., Murphy, K., Moloney, G.M., Cryan, J.F., Dinan, T.G., Ross, R.S., and Stanton, C. (2017). Deficiency of essential dietary n-3 PUFA disrupts the caecal microbiome and metabolome in mice. Br. J. Nutr. *118*, 959–970.

Santillan, E., Phua, W.X., Constancias, F., and Wuertz, S. (2020). Sustained organic loading disturbance favors nitrite accumulation in bioreactors with variable resistance, recovery and resilience of nitrification and nitrifiers. Sci. Rep. *10*, 21388.

Schliep, K.P. (2011). phangorn: phylogenetic analysis in R. Bioinformatics *27*, 592–593.

Schyns, J., Bai, Q., Ruscitti, C., Radermecker, C., De Schepper, S., Chakarov, S., Farnir, F., Pirottin, D., Ginhoux, F., Boeckxstaens, G., et al. (2019). Non-classical tissue monocytes and two functionally distinct populations of interstitial macrophages populate the mouse lung. Nat. Commun. *10*, 3964.

Simó, C., and García-Cañas, V. (2020). Dietary bioactive ingredients to modulate the gut microbiota-derived metabolite TMAO. New opportunities for functional food development. Food Funct. *11*, 6745–6776.

Song, Y., Malmuthuge, N., Steele, M.A., and Guan, L.L. (2018). Shift of hindgut microbiota and microbial short chain fatty acids profiles in dairy calves from birth to pre-weaning. FEMS Microbiol. Ecol. *94*, fix179.

Spiel, A.O., Gilbert, J.C., and Jilma, B. (2008). Von Willebrand factor in cardiovascular disease: focus on acute coronary syndromes. Circulation *117*, 1449–1459.

Stivala, S., Gobbato, S., Infanti, L., Reiner, M.F., Nicole Bonetti, N.R., Meyer, S.C., Camici, G.G., Lüscher, T.F., Buser, A., and Beer, J.H. (2017). Amotosalen/ultraviolet A pathogen inactivation technology reduces platelet activatability, induces apoptosis and accelerates clearance. Haematologica *102*, 1650–1660.

Stivala, S., Reiner, M.F., Lohmann, C., Lüscher, T.F., Matter, C.M., and Beer, J.H. (2013). Dietary alpha-linolenic acid increases the platelet count in ApoE-/- mice by reducing clearance. Blood *122*, 1026–1033.

Stivala, S., Sorrentino, S., Gobbato, S., Bonetti, N.R., Camici, G.G., Lüscher, T.F., Medalia, O., and Beer, J.H. (2020). Glycoprotein Ib clustering in platelets can be inhibited by α-linolenic acid as revealed by cryo-electron tomography. Haematologica *105*, 1660–1666.

Tabata, T., Yamashita, T., Hosomi, K., Park, J., Hayashi, T., Yoshida, N., Saito, Y., Fukuzawa, K., Konishi, K., Murakami, H., et al. (2021). Gut microbial composition in patients with atrial fibrillation: effects of diet and drugs. Heart Vessel. *36*, 105–114.

Tang, W.H., Wang, Z., Levison, B.S., Koeth, R.A., Britt, E.B., Fu, X., Wu, Y., and Hazen, S.L. (2013). Intestinal microbial metabolism of phosphatidylcholine and cardiovascular risk. N. Engl. J. Med. *368*, 1575–1584.

Tang, W.H.W., Li, D.Y., and Hazen, S.L. (2019). Dietary metabolism, the gut microbiome, and heart failure. Nat. Rev. Cardiol. *16*, 137–154.

Tjärnlund-Wolf, A., Brogren, H., Lo, E.H., and Wang, X. (2012). Plasminogen activator inhibitor-1 and thrombotic cerebrovascular diseases. Stroke *43*, 2833–2839.

Trøseid, M., Andersen, G.Ø., Broch, K., and Hov, J.R. (2020). The gut microbiome in coronary artery disease and heart failure: current knowledge and future directions. EbioMed *52*, 102649.

Turnbaugh, P.J., Bäckhed, F., Fulton, L., and Gordon, J.I. (2008). Diet-induced obesity is linked to marked but reversible alterations in the mouse distal gut microbiome. Cell Host. Microbe *3*, 213–223.

Verhaar, B.J.H., Collard, D., Prodan, A., Levels, J.H.M., Zwinderman, A.H., Bäckhed, F., Vogt, L., Peters, M.J.L., Mulle, M., Nieuwdorp, M., et al. (2020). Associations between gut microbiota, faecal short-chain fatty acids, and blood pressure across ethnic groups: the HELIUS study. Eur. Heart J. *00*, 1–9.

Wang, B., Kong, Q., Li, X., Zhao, J., Zhang, H., Chen, W., and Wang, G. (2020). A high-fat diet increases gut microbiota biodiversity and energy expenditure due to nutrient difference. Nutrients *12*, 3197.

Wang, Y., Xu, L., Liu, J., Zhu, W., and Mao, S. (2017). A high grain diet dynamically shifted the composition of mucosa-associated microbiota and induced mucosal injuries in the colon of sheep. Front. Microbiol. *8*, 1–13.

Wang, Z., Roberts, A.B., Buffa, J.A., Levison, B.S., Zhu, W., Org, E., Gu, X., Huang, Y., Zamanian-Daryoush, M., Culley, M.K., et al. (2015). Non-lethal inhibition of gut microbial trimethylamine production for the treatment of atherosclerosis. Cell *163*, 1585–1595.

Wang, Z., Klipfell, E., Bennett, B.J., Koeth, R., Levison, B.S., DuGar, B., Feldstein, A.E., Britt, E.B., Fu, X., Chung, Y.M., et al. (2011). Gut flora metabolism of phosphatidylcholine promotes cardiovascular disease. Nature *472*, 57–63.

Watson, H., Mitra, S., Croden, F.C., Taylor, M., Wood, H.M., Perry, S.L., Spencer, J.A., Quirke, P., Toogood, G.J., Lawton, C.L., et al. (2018). A randomised trial of the effect of omega-3 polyunsaturated fatty acid supplements on the human intestinal microbiota. Gut *67*, 1974–1983.

Winnik, S., Lohmann, C., Richter, E.K., Schafer, N., Song, W.L., Leiber, F., Mocharla, P., Hofmann, J., Klingenberg, R., Boren, J., et al. (2011). Dietary alpha-linolenic acid diminishes experimental atherogenesis and restricts T cell-driven inflammation. Eur. Heart J. *32*, 2573–2584.

Witkowski, M., Weeks, T.L., and Hazen, S.L. (2020). Gut microbiota and cardiovascular disease. Circ. Res. *127*, 553–570.

Wright, E.S. (2016). Using DECIPHER v2.0 to analyze big biological sequence data in R. R. J. *8*, 352–359.

Wu, N., Tong, S., Xiang, Y., Wu, L., Xu, B., Zhang, Y., Ma, X., Li, Y., Song, Z., and Zhong, L. (2015). Association of hemostatic markers with atrial fibrillation: a meta-analysis and meta-regression. PLoS One *10*, e0124716.

Yamamoto, K., Takeshita, K., Kojima, T., Takamatsu, J., and Saito, H. (2005). Aging and plasminogen activator inhibitor-1 (PAI-1) regulation: implication in the pathogenesis of thrombotic disorders in the elderly. Cardiovasc. Res. *66*, 276–285.

Yan, Y., Jiang, W., Spinetti, T., Tardivel, A., Castillo, R., Bourquin, C., Guarda, G., Tian, Z., Tschopp, J., and Zhou, R. (2013). Omega-3 fatty acids prevent inflammation and metabolic disorder through inhibition of NLRP3 inflammasome activation. Immunity *38*, 1154–1163.

Younge, N., Yang, Q., and Seed, P.C. (2017). Enteral high fat-polyunsaturated fatty acid blend alters the pathogen composition of the intestinal microbiome in premature infants with an enterostomy. J. Ped. *181*, 93–101.

Yu, J., Zhang, T., Gao, X.M., Xue, C., Xu, J., and Wang, Y. (2017). Fish oil affects the metabolic process of trimethylamine N-oxide precursor through trimethylamine production and flavin-containing monooxygenase activity in male C57BL/6 mice. RSC Adv. *7*, 56655–56661.

Yuan, G., Zhang, Z., Gao, X., Zhu, J., Guo, W., Wang, L., Ding, P., Jiang, P., and Li, L. (2020). Gut microbiota-mediated tributyltin-induced metabolic disorder in rats. RSC Adv. *10*, 43619–43628.

Zeisel, S.H., and Warrier, M. (2017). Trimethylamine N-oxide, the microbiome, and heart and kidney disease. Annu. Rev. Nutr. *37*, 157–181.

Zhang-Sun, W., Augusto, L.A., Zhao, L., and Caroff, M. (2015). *Desulfovibrio desulfuricans* isolates from the gut of a single individual: structural and biological lipid A characterization. FEBS Lett. *589*, 165–171.

Zhao, Z.H., Xin, F.Z., Xue, Y., Hu, Z., Han, Y., Ma, F., Zhou, D., Liu, X.L., Cui, A., Liu, Z., et al. (2019). Indole-3-propionic acid inhibits gut dysbiosis and endotoxin leakage to attenuate steatohepatitis in rats. Exp. Mol. Med. *51*, 103.

Zheng, C., Huang, K., Zhao, C., Xu, W., Sheng, Y., Luo, Y., and He, X. (2018). Procyanidin attenuates weight gain and modifies the gut microbiota in high fat diet induced obese mice. J. Func. Food *49*, 362–368.

Zhu, B., Zhai, Y., Ji, M., Wei, Y., Wu, J., Xue, W., Tao, W.W., and Wu, H. (2020a). *Alisma orientalis* beverage treats atherosclerosis by regulating gut microbiota in *ApoE*$^{-/-}$ mice. Front. Pharmacol. *11*, 570555.

Zhu, C., Sawrey-Kubicek, L., Bardagjy, A.S., Houts, H., Tang, X., Sacchi, R., Randolph, J.M., Steinberg, F.M., and Zivkovic, A.M. (2020b). Whole egg consumption increases plasma choline and betaine without affecting TMAO levels or gut microbiome in overweight postmenopausal women. Nutr. Res. *78*, 36–41.

Zhu, W., Gregory, J.C., Org, E., Buffa, J.A., Gupta, N., Wang, Z., Li, L., Fu, X., Wu, Y., Mehrabian, M., et al. (2016). Gut microbial metabolite TMAO enhances platelet hyperreactivity and thrombosis risk. Cell *165*, 111–124.

Zhu, W., Li, W., and Silverstein, R.L. (2012). Advanced glycation end products induce a prothrombotic phenotype in mice via interaction with platelet CD36. Blood *119*, 6136–6144.

Ziętak, M., Kovatcheva-Datchary, P., Markiewicz, L.H., Sta° hlman, M., Kozak, L.P., and Bäckhed, F. (2016). Altered microbiota contributes to reduced diet-induced obesity upon cold exposure. Cell. Metab. *23*, 1216–1223.

Zou, J., Shen, Y., Chen, M., Zhang, Z., Xiao, S., Liu, C., Wan, Y., Yang, L., Jiang, S., Shang, E., et al. (2020). Lizhong decoction ameliorates ulcerative colitis in mice via modulating gut microbiota and its metabolites. App. Microbiol. Biotechnol. *104*, 5999–6012.

Zuo, K., Li, J., Xu, Q., Hu, C., Gao, Y., Chen, M., Hu, R., Liu, Y., Chi, H., Yin, Q., et al. (2019). Dysbiotic gut microbes may contribute to hypertension by limiting vitamin D production. Clin. Cardiol. *42*, 710–719.

STAR★METHODS

KEY RESOURCES TABLE

REAGENT or RESOURCE	SOURCE	IDENTIFIER
Antibodies		
Anti-mouse CD62P (P-Selectin) PE (Clone Wug.E9)	Emfret Analytics	Cat#: M130-2
Anti-mouse integrin αIIbβ3 (GPIIb/IIIa, CD41/CD61)-PE (Clone: Leo.F2)	Emfret Analytics	Cat#: M025-2; RRID:AB_2833084
DyLight 649 anti- mouse CD42b (GPIb) (Clone: Xia.G5)	Emfret Analytics	Cat#: M040-3
Alexa Fluor 647 donkey anti-mouse	Jackson Immunoresearch	Cat#: 712-605-153; RRID:AB_2340862
Biological samples		
Mouse intracardiac whole blood	Animal Experimental Trials	NA
Mouse plasma	Animal Experimental Trials	NA
Mouse feces	Animal Experimental Trials	NA
Chemicals, peptides, and recombinant proteins		
Special ALA diet	Research Diets	Cat#: D12021003, -03Y, - 04
Standard chow diet	Research Diets	Cat#: D11112201
NaCl	Sigma-Aldrich	Cat#: S9888
KCl	Sigma-Aldrich	Cat#: P9333
Sodium citrate	Sigma-Aldrich	Cat#: 1613859
Glucose	Sigma-Aldrich	Cat#: G8270
Sucrose	Sigma-Aldrich	Cat#: S0389
HEPES	Sigma-Aldrich	Cat#: H3375-500
$MgCl_2$ hexahydrate	Sigma-Aldrich	Cat#: M2670
$NaHCO_3$	Sigma-Aldrich	Cat#: S-6297
PBS	Gibco	Cat#: 10010023
BSA	Sigma-Aldrich	Cat#: A7906
Calcein AM	Enzo Life Science	Cat#: ENZ-52002
Von Willebrand factor	Hematologic Technologies Inc.	Cat#: HCVWF-0190
Thrombin	Sigma-Aldrich	Cat#: T1063-50UN
ADP	Chrono-Log	Cat#: 384
TRAP-6	Bachem	Cat#: 4017752.0005
Equine tendon collagen	Chrono-Log	Cat#: 385
EDTA	Sigma-Aldrich	Cat#: E5134
Critical commercial assays		
Proteome profiler mouse XL cytokine array	R&D Systems	Cat#: ARY028
Mouse TNF-α quantikine HS ELISA kit	R&D Systems	Cat#: MHSTA50
Lipopolysaccharide ELISA	Cusabio	Cat#: CSB-E13066m
Nextera XT DNA sample preparation kit	Illumina	Cat#: FC-131
Nextera index kit	Illumina	Cat#: FC-131
Deposited data		
16S rRNA gene amplicon sequencing data	This paper	[SRA]: [SUB8478241]
Project data	This paper	[Mendeley code]: [https://doi.org/10.17632/cx447gy6ps.1]

(*Continued on next page*)

Continued

REAGENT or RESOURCE	SOURCE	IDENTIFIER
Experimental models: Organisms/Strains		
Mouse: C57BL/6J	The Jackson Laboratory	Cat#000664; RRID:IMSR_JAX:000664
Oligonucleotides		
Barcoded PCR primer sequences	Please see Table S3	Please see Table S3
Software and algorithms		
Prism (version 8)	GraphPad	NA
DADA2 R version 1.14.1	BiocManager	https://benjjneb.github.io/dada2/dada-installation.html
DECIPHER R version 2.14.0	BiocManager	https://www.bioconductor.org/packages/release/bioc/html/DECIPHER.html
Phangorn R version 2.5.5	CRAN	https://cran.r-project.org/web/packages/phangorn/index.html
Phyloseq R version 1.32	Github	https://github.com/joey711/phyloseq
MultiQuant	SCIEX	NA
EZChrom software	Agilent	NA

RESOURCE AVAILABILITY

Lead contact

Further information and requests for resources and reagents should be directed to and will be fulfilled by the Lead Contact, Jürg H. Beer (hansjuerg.beer@ksb.ch).

Materials availability

This study did not generate new unique reagents.

Data and code availability

- All bioinformatic data from microbial metagenomic analysis in this paper were obtained from BiocManager, CRAN, and GitHub, and all data from LC–MS/MS analysis of plasma TMAO, choline, and betaine were caught from SCIEX, as indicated in the Method Details and are included in the key resources table.
- The raw 16S rRNA gene Amplicon sequencing datasets generated during this study have been deposited on the Sequence Read Archive (SRA) database (accession number: SUB8478241).
- Original data for all figures in the paper that enable investigators to reproduce the data have been uploaded to Mendeley (code: https://doi.org/10.17632/cx447gy6ps.1). Any additional information required to reanalyze the data reported in this paper is available from the lead contact upon request.

EXPERIMENTAL MODEL AND SUBJECT DETAILS

7-9 week old wild-type C57BL/6J male mice were purchased from the Jackson Laboratory and maintained in our facilities for specific times [In these studies, male mice were utilized to minimize any possible effect of sex and hormonal differences on gut microbiota composition during aging and on ALA pharmacokinetics and pharmacodynamics]. All mice were individually housed in controlled environments in plexiglass cages under a strict 12 hr:12 hr light/dark cycles at 23 $\pm$ 1°C and fed standard chow diet (19% Protein, 61% Carbohydrate and 7% Fat, #D11112201, Research Diets, New Brunswick, NJ, USA) for specific time until 8–12 weeks of age. Mice had access to drinking water and food *ad libitum*. Animal care and experimentation were in accordance to the Directive 2010/63/EU of the European Parliament and of the Council of 22 September 2010 on the protection of animals used for scientific purposes. All animal model studies were approved by the Institutional Animal Care and Use Committee at University of Zurich.

Next, one group of 8-12-week old mice was daily fed a standard chow diet (#D11112201) and two groups of mice were daily fed special diets, one group receiving a diet containing high dose (7.3%) of ALA and the other receiving low (0.03%) ALA (Table S2; 19% Protein, 50% Carbohydrate and 14% Fat, #D12021004, -03, −03Y, Research Diets, New Brunswick, NJ, USA) (as we utilized and described previously; Reiner et al., 2017; Stivala et al., 2013; Holy et al., 2011), for >16 months until >18 months of age. Feces and blood samples were collected from 8 to 12-week old mice, as young state, and from >18-month old mice, as old state. Fecal samples were quickly stored in −80°C for further 16 rRNA sequencing/metagenomic analyses and quantification of short-chain fatty acids. Blood samples were taken, and gently used for platelet aggregometry, *ex vivo* thrombosis experiments, plasma isolation for proteome profiler array, ELISA, and quantification of microbial metaorganismal metabolite TMAO, platelet flow cytometry, and blood count. Notably, the ALA-rich diet has been tolerable and non-toxic for the animals on a lifelong feeding. The animals were monitored for body weight, hemodynamics (systolic, diastolic, and mean blood pressure), and cardiac parameters (ejection fraction and fractional shortening) during their lifespan. Data showed no significant differences at week 12 and month >18 of their age (Data not shown).

METHOD DETAILS

Platelet-rich plasma and washed platelet preparation

PRP and washed platelets were prepared as previously described (Stivala et al., 2017). Whole blood was collected by intracardiac puncture from old (>18-month-old) or young (2-3-month-old) mice under different treatments using anticoagulant sodium citrate (0.109 M). PRP was isolated by centrifuging at 125 *g* for 8 min at room temperature, and washed with 300 μL platelet wash buffer (140 mM NaCl, 5 mM KCl, 12mM sodium citrate, 10 mM glucose, and 12.5 mM sucrose, pH 6.0), and centrifuged again at 860 *g* for 5 min. The platelet pellet was then re-suspended in 200 μL final buffer containing 10 mM HEPES, 140 mM NaCl, 3 mM KCl, 0.5 mM $MgCl_2$ hexahydrate, 0.5 mM $NaHCO_3$, and 10 mM glucose (pH 7.4) for platelet flow cytometric analysis.

Blood analysis

Mice were fasted overnight before blood samples were drawn using EDTA as anticoagulant. Total blood cell count was performed on a ScilVet ABCplus (Horiba, Kyoto, Japan).

Platelet aggregometry assay

Impedance platelet aggregometry assays were performed as previously described (Stivala et al., 2020). In brief, whole blood was collected from old (>18-month-old) or young (2-3-month-old) mice under different treatments using sodium citrate (0.109 M). PRPs were then prepared and maintained with constant stirring (600 rpm) at 37°C on a platelet aggregometer (Chrono-Log, Havertown, PA, USA). Platelet aggregation was initiated by stimulation with ADP (1.25, 2.5, and 5 μM; Chrono-log, Havertown, PA, USA) or equine tendon collagen (2.5, 5, and 10 μg/mL; Chrono-log, Havertown, PA, USA) or TRAP-6 (1.5, 3, and 5 μM; Bachem, Switzerland). Platelet aggregation was expressed as maximal aggregation, lag time, and slope (inclination), and calculated by the AGGRO/LINK software (Chrono-Log).

Whole blood *ex vivo* thrombosis assay

Microfluidic shear flow experiments were performed using the Bioflux Microfluidics System (Fluxion Biosciences, San Francisco, CA, USA) (Stivala et al., 2020). Each micro channel of a 24-well plate was coated with human vWF (100 ug/ml, Hematologic Technologies Inc., USA) and placed at room temperature for 1 hr. Before use each channel was washed with 1x PBS containing Ca^{2+} and Mg^{2+}, and blocked with 0.1% BSA for 10 min. Whole blood collected from mice fluorescently labeled with Calcein AM (4μM final concentration, Enzo Life Science, USA). Blood was then perfused over chambers coated with vWF at low (10 dynes/cm^2) or high (100 dynes/cm^2) physiological shear rates using a multi-channel microfluidic device for 5 min. Platelet adhesion to vWF coating was monitored and images were captured every 10 s using a 10x/0.22 NA objective lens on an inverted microscope (EVOS XL Core Cell Imaging System, Invitrogen). Platelet adherence to the vWF surface and calcein AM stained thrombi was then quantified using Bioflux software, and expressed as platelet-covered area (μm^2).

Platelet flow cytometry

Flow cytometric assays of washed platelets from old or young mice treated with either low or high ALA were performed as previously described (Stivala et al, 2017, 2020). Washed platelets were stimulated with 0.1

and 0.5 U/ml thrombin (Sigma-Aldrich, St. Louis, MO, USA) or vehicle for 10 min, fixed with 4% paraformaldehyde for 15 min, and then incubated with 1% BSA in PBS containing an antibody against GPIb or active integrin $\alpha_{IIb}\beta_3$ (GP IIb/IIIa) or P-selectin (all from Emfret Analytics, Eibelstadt, Germany) in the dark for 20 min. Samples were washed three times in 1% BSA in PBS and then incubated with relevant secondary antibodies (1:250, Jackson Immunoresearch, West Grove,PA, USA) for 30 min. Data were acquired on an FACS LSR Fortessa flow cytometer (BD Biosciences) and analyzed using FlowJo v10 software.

Proteome profiler array

Whole blood samples were centrifuged at 125 *g* for 8 min at room temperature for plasma isolation, as previously described (Holy et al., 2011). For each experimental condition, plasma were tested for the presence of procoagulant factors tissue factor and plasminogen activator inhibitor-1, as well as inflammatory cytokines and chemokinesusing a proteome profiler mouse XL cytokine array (R&D Systems), according to manufacturer instructions (Schyns et al., 2019). Results were visualized using an Amersham Imager 600 (GE Healthcare Europe GmbH) and analyzed using ImageJ software. Values are normalized and expressed as relative pixel values.

ELISA of mice plasma

Plasma TNF-α and lipopolysaccharide (LPS) levels were quantified in accordance with the manufacturer's instruction (Thermo Fisher Scientific, Waltham, MA, USA for TNF-α; Cusabio, Houston, TX, USA for LPS). Briefly, microtiter plates were coated with anti-TNF-α and anti-LPS antibodies. Sodium citrate (0.109 M) anticoagulated plasma was added and incubated for 2 hr at room temperature. Biotinylated antibody was then added and precisely washed 1 hr after incubation. Following 1 hr incubation with avidin-conjugated Horseradish Peroxidase (HRP), TMB substrate was added to each plate and incubated for 30 min in the dark. Optical density was determined at 450 nm and subtracted from absorbance at 540 nm. Finally, plasma TNF-α (pg/mL) and LPS concentration (ng/mL) was calculated according to a standard curve.

LC–MS/MS analysis of mouse plasma samples

Quantification of TMAO, choline, and betaine in plasma samples were similar to that described previously (Reiner et al., 2019; Zhu et al., 2016; Mueller et al., 2015) with minor validated modifications. Briefly, 400 μL of an internal standards of TMAO-d9 (1 μM), choline 1 μM, and betaine (1 μM) were added, vortexed and centrifuged at 11,700 g for 10 min at 4°C. Supernatants were obtained and separated on an Accucore hydrophilic interaction chromatography (HILIC) column (50 × 2.1mm, 2.6 μm; Thermo Fisher Scientific, Reinach, Switzerland) under acidic conditions. The QTRAP 6500 hybrid instrument (Sciex) was operated with electrospray ionization in positive ion mode with the following transitions: 76.1→59.1 (quantifier), 76.1→42.1 (qualifier 1), 76.1→56.2 (qualifier 2) for TMAO, 104.0→60.15 for choline, and 85.1→68.1 for betaine. Data were processed using MultiQuant (Sciex) software.

16S rRNA gene amplicon sequencing and bioinformatic processing

Fecal pellets were immediately preserved at −80°C for further extraction of fecal nucleic acid using Fecal genomic extraction kit according to the manufacturer's instructions (Qiagen). To elucidate whether transcriptional activity of gut microbiota contribute to the synthesis of TMAO and SCFAs, and the secretion of procoagulant factors TF and PAI-1, we performed sequencing of the fecal microbes in young or old mice fed a diet containing low or high doses of ALA (n = 5–9). Metabarcoding libraries were generated using a two-step PCR approach as recommended by Illumina. The first PCR was performed to amplify V3-V4 16S gene region using primers 341F (5′-CCT ACG GGN GGC WGC AG -3′) and 805R (5′-GAC TAC HVG GGT ATC TAA TCC -3′). Samples were then indexed using Nextra indices according to manufacturer's instruction (Illumina), and sequencing was performed with paired-end reads on Illumina MiSeq platform and a v2 500 cycles kit. Both negative and positive (e.g. mock community) were included in sequencing to assess quality of the reads and identification of adapter contamination.

Bioinformatic analysis was performed using DADA2 R package version 1.14.1, as previously described (Santillan et al., 2020; Callahan et al., 2016) [DADA2 enables the exact ASVs inference providing distinct benefits over traditional OTU clustering methods]. In brief, reads were truncated after 227 and 223 nucleotides for forward and reverse reads, respectively. Reads with expected error rates higher than 4 and 5 for forward and reverse reads were subsequently removed. The resulting ASV abundance table was filtered, and ASV inference was then performed using a pseudo-pooling strategy. Forward and reverse reads were

then merged with a minimum overlap of 10 nucleotides and chimeric sequences were identified and removed. Taxonomy was assigned to ASVs using methods implemented in DADA2 using SILVA_138 reference database (Glöckner et al., 2017). Phylogenetic relativeness of ASVs was characterized by multiple alignments of ASV sequences using DECIPHER R package version 2.14.0 (Wright 2016). The phylogenetic tree was then constructed, and a GTR + G + I (generalized time reversible with gamma rate variation) maximum likelihood tree was then matched using phangorn R package version 2.5.5 (Schliep 2011).

Quantitative SCFA analysis

Feces were collected and quickly stored at −80°C for further quantification of SCFA, including acetate and propionate, using high-performance liquid chromatography equipped with a refractive index detector (HPLC-RI) (Li et al., 2019; Poeker et al., 2019). In brief, feces were initially weighed, mixed with H_2SO_4 10 mM, and then homogenized. The fecal suspension was centrifuged for at 6000 rpm for 20 min at 4°C. Subsequently, the supernatant was filtered for further HPLC-RI analysis. Separation was carried out with a LaChrom HPLC-System (Merck-Hitachi, Japan) using a SecurityGuard Cartridges Carbo-H (4 × 3.0 mm) (Phenomenex Inc., Torrance CA, USA) connected to a Rezex ROA-Organic Acid H^+ column (300 × 7.8 mm; Phenomenex Inc.). Samples (40 μL injection) were eluted at 40°C under isocratic conditions (10 mM H_2SO_4, flow rate 0.4 mL/min), and analytes were quantified using a refractive index detector L-2490 (Merck-Hitachi). Data were processed using EZChrom software.

QUANTIFICATION AND STATISTICAL ANALYSIS

Detailed statistical methods are described in the supplemental information. Statistical differences were assessed by paired, two-tailed Student's t-test or one-way Analysis of variance (ANOVA) followed by Tukey's multiple comparison post-test. At least three independent triplicated experiments have been performed for each experimental set-up. Statistical analysis was performed using GraphPad Prism software version 8.0 (GraphPad Software, La Jolla, CA, USA), R v1.26.1 (Vienna, Austria, 2017), and vegan v2.5-5. Spearman rank correlation was used to analyze association between quantitative variables. Data are expressed as mean ± SD, and $p < 0.05$ was defined as statistically significant, indicated as *; $p < 0.01$ as **; $p < 0.001$ as ***, and $p < 0.0001$ as ****.

ASV count table, phylogenetic tree and taxonomic assignments were imported in R and loaded into a phyloseq object for data handling (McMurdie and Holmes 2013). ASV table was rarefied to an even number of XXX sequences per sample in order to apply robust diversity quantifications (Wright 2016). Bacterial community structure (beta-diversity) was analyzed using Atchinson distance and visualized using Principal Coordinate Analysis (PCoA). Bacterial communities were also characterized using alpha-diversity indices Shannon's index, Richness (Observed), as well as, Faith's Phylogenetic diversity and SES.MPD (NRI), which reflect phylogenetic clustering or distribution of the ASV. Differences were tested using Kruskal-Wallis and PERMANOVA statistical methods for alpha- and beta-diversity, respectively. Differential abundance testing was performed using negative binomial tests as implemented in DESeq2 (Anders and Huber 2010). Multiple comparisons and associated p values were FDR corrected.